NORWEGIAN JOURNAL OF GEOLOGY
https://dx.doi.org/10.17850/njg103-1-2

GEOLOGICAL SOCIETY OF NORWAY

The Hambergfjellet Formation on Bjørnøya – sedimentary response to early Permian tectonics on the Stappen High

Sten-Andreas Grundvåg[1,2], Mathias Skaar Strand[3], Christian Paulsen[3], Bjørn Tore Simonsen[4], Jostein Røstad[3], Atle Mørk[3], Mai Britt E. Mørk[3]

[1]*Department of Geosciences, UiT The Arctic University of Norway, PO Box 6050 Langnes, 9037 Tromsø, Norway*
[2]*Department of Arctic Geology, University Centre in Svalbard, P.O. Box 156, 9171, Longyearbyen, Norway*
[3]*Department of Geoscience and Petroleum – NTNU, Trondheim, 7031 Trondheim, Norway*
[4]*Vågslien 58, 5013 Tertnes, Norway.*

E-mail corresponding author (Sten-Andreas Grundvåg) sten-andreas.grundvag@uit.no

Keywords:
- *Upper Palaeozoic*
- *Bjarmeland Group*
- *Carbonate platform*
- *Svalbard*
- *Barents Shelf*

Received:
9. September 2022

Accepted:
8. December 2022

Published online:
14. February 2023

On Bjørnøya, the exhumed crest of the Stappen High, the lower Permian (Cisuralian) Hambergfjellet Formation represents the only exposed part of the Bjarmeland Group carbonate platform, which occurs widely elsewhere in the subsurface of the Barents Shelf. A complex stratigraphic architecture has earlier been noted for the Hambergfjellet Formation and thickness estimates range from c. 50 to more than 100 m. Moreover, the unit lacks a formal type section, which hampers accurate regional correlations and comparisons. In this stratigraphic study, we integrate new field observations and microfacies analysis with data from previous work to present a composite section which is proposed as the type section for the Hambergfjellet Formation. Four internal units are recognized. Units A and B (post ?late Asselian–?Sakmarian), which consist of mixed carbonate and siliciclastic rocks interpreted to be of shallow marine origin, are restricted to a series of fault-bounded basins defined by gently rotated basement fault blocks. Locally, units A and B onlap or truncate lowermost Permian strata and appear to transgressively fill in antecedent topography presumably created during Sakmarian uplift and erosion of the Stappen High. The distorted character of unit A suggests that slumping was an important process during the initial phase of infilling, amid or soon after transgression. Unit C (?Sakmarian–?early Artinskian) is a thick-bedded, sheet-like limestone unit which contains fauna elements consistent with deposition on a warm-water carbonate platform occasionally subject to subaerial exposure. Unit D (late Artinskian) is a brachiopod-dominated, fusulinid-bearing, bioclastic limestone unit deposited on a fully marine, transitional warm-temperate to cool-water carbonate platform which developed during a late Artinskian circum-Arctic transgression. The unit only occurs in the eastern part of the outcrop belt on southern Bjørnøya due to fault-controlled tilting and peneplanation prior to deposition of the Miseryfjellet Formation (Kungurian–Wordian) limestones. Distinct evidence, including breccia pipes, points to prolonged exposure and karstification of the Hambergfjellet Formation carbonate platform prior to

Grundvåg, S.-A., Strand, M.S., Paulsen, C., Simonsen, B.T., Røstad, J., Mørk, A. & Mørk, M.B.E. 2023: The Hambergfjellet Formation on Bjørnøya – sedimentary response to early Permian tectonics on the Stappen High. *Norwegian Journal of Geology 103,* 202302. https://dx.doi.org/10.17850/njg103-1-2

transgression and submergence of the Stappen High in the middle to late Permian (Guadalupian). The presence of angular and highly diachronous unconformities at the base and top of the formation, a series of small grabens, internal dip variations, as well as a conspicuous north to north-eastward thinning manifest tectonism pre-dating the late Permian extensional event along the western Barents Shelf margin. As such, we shed a new light on the Permian tectonostratigraphic evolution of the Stappen High.

Introduction

The upper Palaeozoic succession of the Barents Shelf includes an ambiguous carbonate-dominated unit of early Permian age (Cisuralian), the Bjarmeland Group, which is widespread across large parts of the shelf with thick deposits particularly on the Bjarmeland and Finnmark platforms (e.g., Larssen et al., 2002; see Fig. 1A for locations). These carbonate rocks have been the target of several exploration

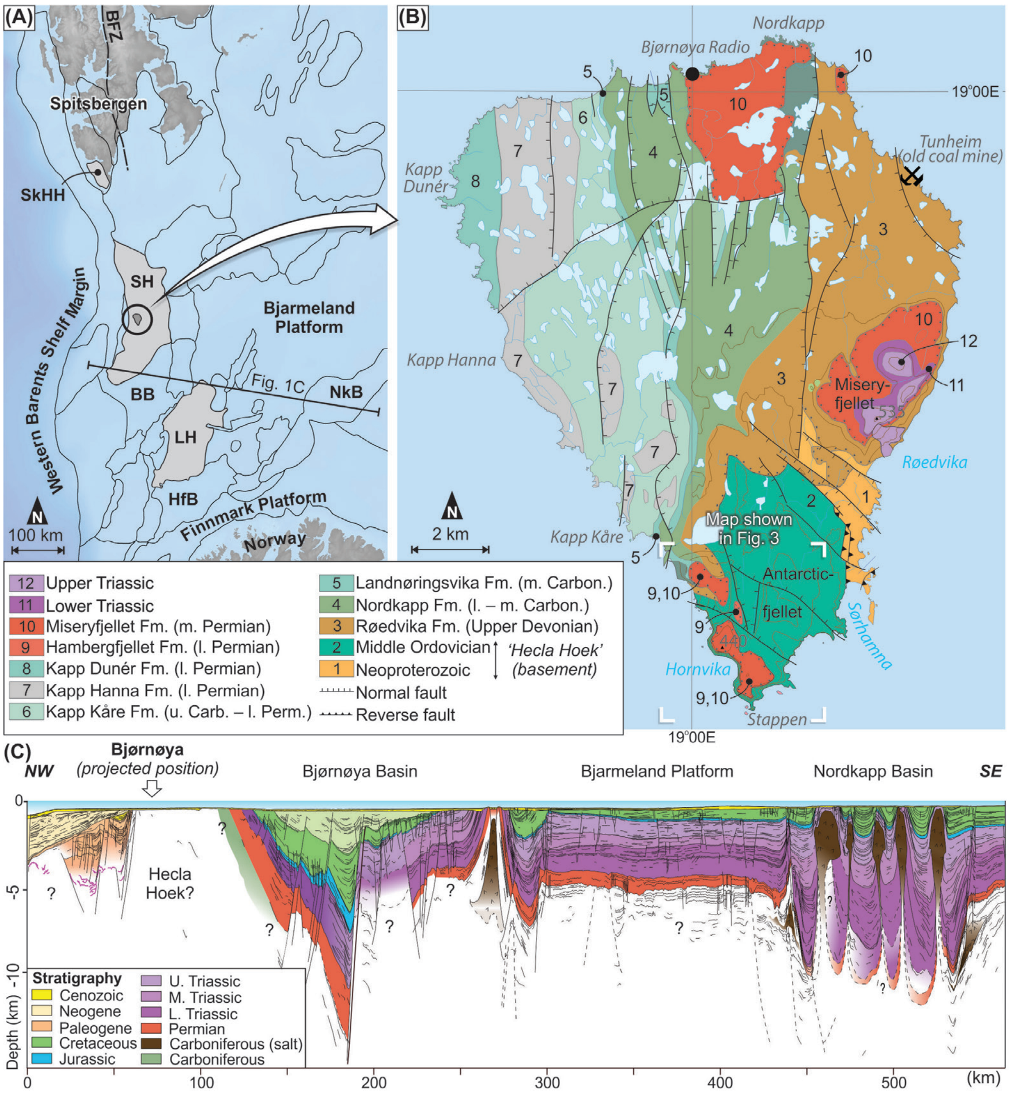

Figure 1. (A) Map of the western Barents Shelf showing the position of Bjørnøya, halfway between Spitsbergen and Norway. Main structural elements as outlined in Henriksen et al. (2011), including the Bjørnøya Basin (BB), Hammerfest (HfB), and Nordkapp (NkB) basins, as well as the Loppa (LH), Stappen High (SH), and Sørkapp–Hornsund (SkHH) highs. (B) Geological map of Bjørnøya. This study investigates the Permian Hambergfjellet Formation (unit 9 on the map). Based on Dallmann & Krasil'ščikov (1996). (C) Geoseismic profile from the Nordkapp Basin across the Bjarmeland Platform to the Stappen High. Bjørnøya represent the tilted and exposed crest of the Stappen High. From Smelror et al. (2009).

campaigns as they may hold some reservoir potential (Stemmerik et al., 1999; Larsen et al., 2002; Di Lucia et al., 2017; Sayago et al., 2018). In the subsurface, seismic data show that the Bjarmeland Group exhibits significant lateral thickness variations onlapping and thinning across structural highs, whereas core data shows that it contains a varied open-marine fossil fauna consisting of brachiopods, bryozoans, crinoids, and siliceous sponges (Bugge et al., 1995; Larssen et al., 2002). The group has been proposed to record the development of an extensive, apparently tectonically stable, cool-water carbonate platform during the early Permian (Stemmerik, 1997; Worsley et al., 2001; Larssen et al., 2002).

On Bjørnøya, which represents the exhumed and truncated crest of the Stappen High (Fig. 1), a part of this group is excellently exposed on the southern tip of the island. Here, the strata, which are assigned to the Hambergfjellet Formation, consist of mixed siliciclastic and carbonate deposits of presumably Sakmarian to Artinskian age (Fig. 2; Horn & Orvin, 1928; Worsley & Edwards, 1976; Worsley et al., 2001). The Hambergfjellet Formation is rich in fauna elements consistent with shallow, high-energy shelf conditions (Gobbett, 1963; Nakrem, 1991a, b; Worsley et al., 2001) and was previously referred to as the *Cora Limestone* due to its high abundance of brachiopods identified as *Productus cora* by Andersson (1899).

Despite previous efforts, there are several discrepancies with respect to the stratigraphic and lateral development of the Hambergfjellet Formation. Thickness estimates, for example, ranges from *c.* 50 m to more than a 100 m (e.g., Worsley & Edwards, 1976; Harland, 1997; Dallmann et al., 1999; Worsley et al., 2001). The formation reportedly wedges out rather abruptly in a north to north-eastward direction, and in their classical cross-section of Bjørnøya, Horn & Orvin (1928) indicated an eastward thinning

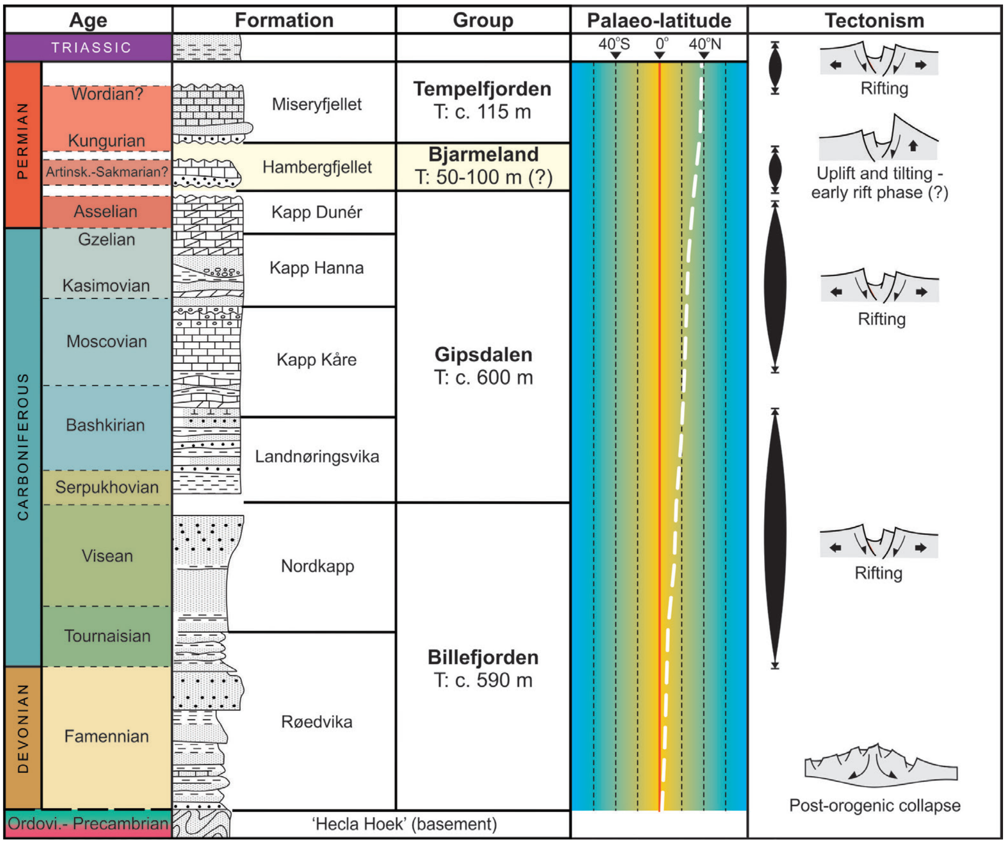

Figure 2. Lithostratigraphic column of Bjørnøya with approximate palaeo-latitudes and main tectonic events affecting the western Barents Shelf and the Stappen High during the late Palaeozoic Era. Compiled from Worsley et al. (2001) and Smelror et al. (2009). The tectonic events are based on Faleide et al. (1984) and Blaich et al. (2017). T – Thickness.

whereby the formation eventually pinches out at the southern tip of Alfredfjellet (Fig. 3A). In contrast, Dallmann & Krasil'ščikov (1996) inferred a constant thickness for the unit across the entire outcrop belt in southern Bjørnøya (Fig. 3B). Simonsen (1991) noted a complex stratigraphic development for the Hambergfjellet Formation, clearly demonstrating that several stratigraphic sections are needed to account for its complexity. Based on this work, Dallmann et al. (1999) suggested a stratotype section for the unit on Hambergfjellet and a hypostratotype section on Alfredfjellet. In their synthesis of the

Figure 3. (A) The classical cross-section by Horn & Orvin (1928) showing the apparent stratigraphic pinch-out of the Hambergfjellet Formation (highlighted in red) across Alfredfjellet in an eastward direction. Lithostratigraphic unit names modified according to the current framework of Dallmann et al. (1999). Rvk – Røedvika Formation, Nkp – Nordkapp Formation, Lnv – Landnøringsvika Formation, HF – Hambergfjellet Formation, MF – Miseryfjellet Formation. (B) Geological map of the study area in the southwestern part of Bjørnøya (from Dallmann & Krasil'ščikov, 1996). The Hambergfjellet Formation (unit 9 on the map) is excellently exposed in the steep and inaccessible coastal cliffs at Alfredfjellet, Hambergfjellet and Fuglefjellet. According to the map, the Hambergfjellet Formation has a sheet-like distribution across the entire outcrop belt. The point of view of the panoramas shown in Figs. 5–8 is indicated. (C) Topographic map (adapted from https://toposvalbard.npolar.no/) showing position of the investigated sections and the digital outcrop model at Alfredfjellet.

sedimentary geology of Bjørnøya, Worsley et al. (2001) presented type sections for the majority of the lithostratigraphic units on the island, apart from the Hambergfjellet Formation. As such, the Hambergfjellet Formation currently lacks a formal type section. All the above stratigraphic inconsistencies need to be clarified, as they have implications for our understanding of the tectono-sedimentary evolution of the Bjarmeland Group and possibly the Permian development of the Stappen High.

Because the Hambergfjellet Formation is typically exposed in steep, inaccessible cliffs, stratigraphic work is a hazardous activity. However, during the summer of 2017, we managed to safely measure and describe the middle part of the Hambergfjellet Formation, although time did not permit a full study of the unit. During a field campaign in the summer of 2020, more locations were visited and described, and with the aid of drone data, multiple sections were tied together. The aim of this paper is to present a composite type section for the Hambergfjellet Formation based on new field observations, extensive photo interpretation, and microfacies analysis integrated with data from previous work. The stratigraphic and lateral development of the unit is extensively documented and thoroughly discussed with respect to the Permian tectonostratigraphic evolution of the Stappen High and nearby basins on the Barents Shelf.

Geological setting

Bjørnøya, which is the southernmost island of the Svalbard archipelago, is located centrally in the Barents Sea, halfway between mainland Norway and Spitsbergen (Fig. 1A). Despite its small size (178 km^2), the island exposes a diverse geological succession (Figs. 1B & 2). An Upper Devonian to Upper Triassic sedimentary succession consisting of siliciclastic strata, including coal-bearing units as well as carbonate rocks, sits on top of a metamorphic to meta-sedimentary basement of Neoproterozoic to Ordovician age (i.e., the Hecla Hoek; Fig. 2). Bjørnøya is the highest point of the Stappen High, representing its tilted and exposed crest (Larssen et al., 2002; Henriksen et al., 2011; Fig. 1C). The Stappen High and its lateral equivalent to the south, the Loppa High, were both positive features during parts of the late Palaeozoic Era, acting as local source areas as well as governing sediment routing along the western shelf margin (e.g., Faleide et al., 1984; Worsley et al., 2001; Henriksen et al., 2011; Blaich et al., 2017; Fig. 4). The Stappen High has undergone multiple phases of fault-related uplift and subsidence, largely controlled by the development of the North Atlantic Rift System with several pronounced extensional phases in the Carboniferous to late Permian (e.g., Faleide et al., 1984; Ritter et al., 1996; Gudlaugsson et al., 1998; Blaich et al., 2017). In the early Permian, the Stappen High was presumably influenced by some minor and localized fault activity (Worsley et al., 2001).

During the Devonian through the Permian, the Barents Shelf and adjacent basins drifted northward from equator to a latitude of approximately 40°N by the end of the Permian (Stemmerik, 1997; Beauchamp & Desrochers, 1997; Worsley et al., 2001; Figs. 2 & 4). The northward drift is recorded in the Upper Palaeozoic sedimentary succession of Svalbard and the Barents Shelf by a regional change from terrestrial coal-bearing clastic rocks of the Upper Devonian to Carboniferous Billefjorden Group through warm-water carbonates and evaporites of the lower Permian Gipsdalen Group to cool-water carbonates and spiculitic cherts of the middle to upper Permian Tempelfjorden Group (Steel & Worsley, 1984; Stemmerik, 1997; Worsley et al., 2001; Larssen et al., 2002). Similar shifts from warm- to cool-water carbonates have also been reported in several adjacent Arctic basins (e.g., NE Greenland and the Sverdrup Basin of Arctic Canada; Beauchamp & Henderson, 1994; Beauchamp & Desrochers, 1997; Stemmerik, 1997).

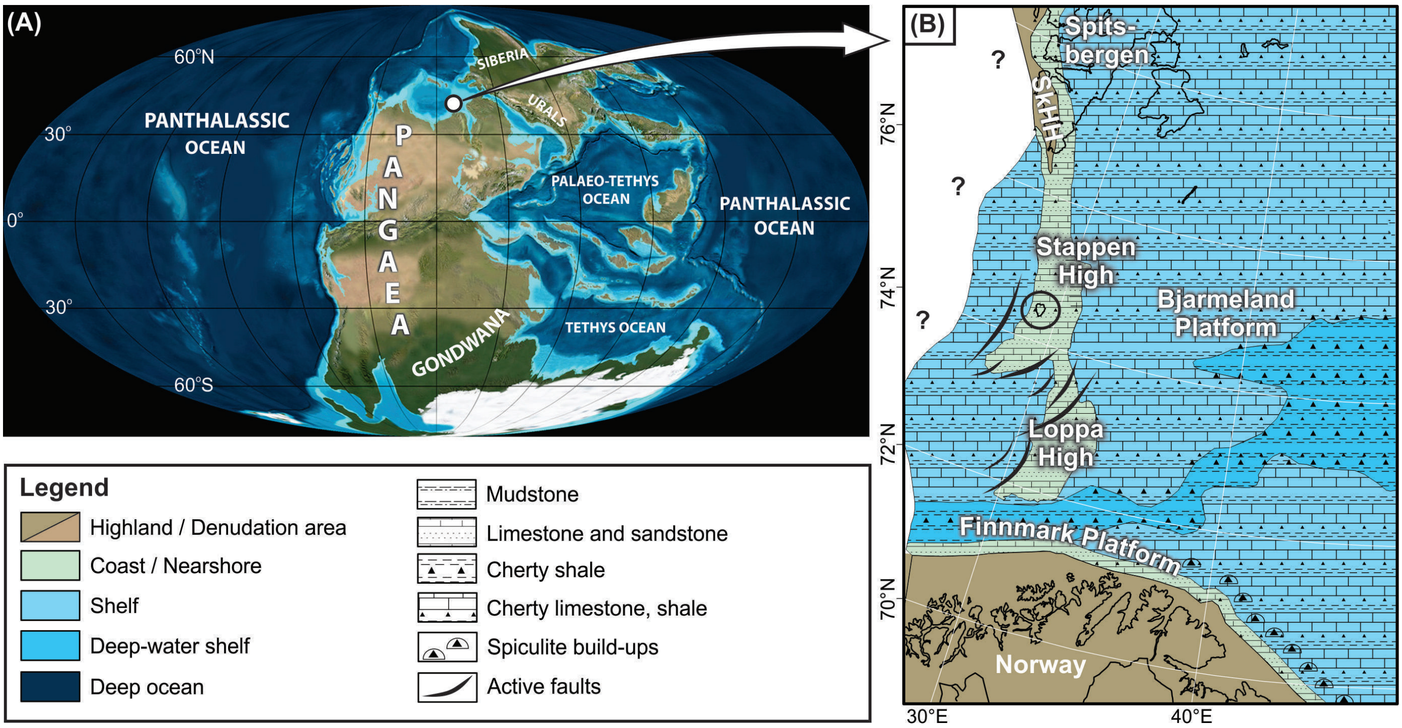

Figure 4. (A) Palaeogeographic reconstruction of the middle Permian (c. 260 Ma, latest Guadalupian Epoch) World showing Bjørnøya's position (white circle) at the northwestern margin of the supercontinent Pangaea where it formed part of an extensive carbonate platform. Modified from Blomeier (2015) based on work by R. Blakey (https://deeptimemaps.com/). (B) Palaeogeographic reconstruction of the Barents Shelf during the middle Permian illustrating shoaling of the carbonate platform across the submerged Stappen and Loppa highs. Due to active faulting along the western margin of the Stappen High, Bjørnøya (encircled) experienced multiple episodes of uplift and subaerial exposure during the Permian. Note that it is the present latitudes and longitudes that are annotated. Compiled from Smelror et al. (2009) and Blaich et al. (2017).

Based on the pioneering work of Andersson (1899) and Horn & Orvin (1928) and after additional fieldwork, Worsley & Edwards (1976) redefined the lithostratigraphy of the sedimentary succession on Bjørnøya. This lithostratigraphic framework was generally retained by Dallmann et al. (1999). However, in the stratigraphic scheme of Cutbill & Challinor (1965) the Hambergfjellet Formation was assigned to the Gipsdalen Group, whereas Dallmann & Krasil'ščikov (1996) referred it to the Tempelfjorden Group, before the unit was eventually formally assigned to the Bjarmeland Group (Dallmann et al., 1999). The latter assignment was based on the similarity to the newly discovered Bjarmeland Group cool-water bioclastic limestones reported in several exploration wells offshore (e.g., Larssen et al., 2002).

Locally, the base of the Bjarmeland Group is a subaerial exposure surface, and the underlying warm-water carbonate platform deposits of the Gipsdalen Group commonly exhibit signs of karstification and freshwater dissolution (e.g., Larssen et al., 2002; Sayago et al., 2012; Ahlborn et al., 2014). The limestones of the Bjarmeland Group, including the Hambergfjellet Formation, started to accumulate during a regional transgression in the middle/late Sakmarian, and is part of a laterally extensive carbonate platform that persisted throughout the Artinskian (e.g., Worsley et al., 2001; Larssen et al., 2002; Stemmerik & Worsley, 2005). Renewed tectonic activity resulted in uplift and tilting of the Hambergfjellet Formation strata, before a supra-regional, middle Permian (Guadalupian) transgression eventually drowned the entire Stappen High, further stimulating prolonged deposition of fully marine, cool-water carbonates and spiculitic cherts of the Tempelfjorden Group across the entire region until the latest Permian (e.g., Stemmerik, 1997; Worsley et al., 2001; Larssen et al., 2002; Stemmerik & Worsley, 2005; Blomeier et al., 2013). On Bjørnøya, the latter group is represented by the middle Permian Miseryfjellet Formation (Kungurian–Wordian), which rests unconformably atop the Hambergfjellet Formation (Worsley & Edwards, 1976; Worsley et al., 2001).

Methods and data collection

The Hambergfjellet Formation is best exposed in the upper part of the *c*. 400–450 m tall, vertical cliffs at the southern to southwestern faces of Alfredfjellet, Hambergfjellet and Fuglefjellet (Figs. 3 & 5). Although the steepness at all these localities makes the unit largely inaccessible, the lateral extent and excellent exposure in the coastal cliffs makes it possible to trace the unit from the seashore and on photo mosaics and characterize its stratigraphic development with high confidence (Fig. 5). The upper part of the formation was measured in 2017 on the southeastern side of Alfredfjellet (logs 17-1 and 17-2; Figs. 5E & 6). A longer section, which spans large parts of the formation, was measured in the exposed cliffs above Skredneset at Alfredfjellet by BTS in 1984 (here referred to as log 84-1; Simonsen, 1991; Fig. 6). Due to its inaccessibility, the upper part of the section was only evaluated from a distance. A digital outcrop model was created from drone photos of the western side of Alfredfjellet (Fig. 7A). This enabled detailed thickness measurements along the otherwise inaccessible outcrop by using the LIME software (see Buckley et al., 2019). Some accessible sections occur in less steep outcrops scattered on the landward-facing slopes of the mountains (Figs. 3C & 7B, C).

The uppermost part of the formation, including the boundary to the overlying Miseryfjellet Formation, is accessible on the eastern side of Hambergfjellet (logs HAM1 and HAM3; Fig. 6) and in a downfaulted block in Ymerdalen (log YMR1; Fig. 6). For stratigraphic comparison, some additional stratigraphic information was also collected from shorter sections on Alfredfjellet, generally covering the lower part of the Miseryfjellet Formation (locations ALF1 to ALF5 in Figs. 3C, 6 & 7C).

During logging of all sections, lithology, bed thickness, grain-sizes, fossils, and trace fossils were noted. When carbonate rocks were encountered, the texture was classified according to Dunham (1962). However, outcrops on Bjørnøya are generally heavily weathered and commonly scree-covered, and the abundance of bird droppings makes field descriptions and recognition of depositional structures and fossils complicated. To assist facies identification, nineteen thin sections made from samples collected at the HAM1 and HAM3 outcrop sections were analysed and subsequently counted. The carbonate classification of Dunham (1962) was used for the microfacies analysis. Body fossils, often occurring as fragments, were identified based on pictures and descriptions from various literature resources (Dunham, 1962; Hanken, 1981; Scholle, 1998; Adams & Mackenzie 1998; Flügel, 2004; Hanken et al., 2010). Fossil grains were divided into non-fusulinid foraminifera, fusulinids, brachiopods, ostracods, bryozoans, and echinoderms. Brachiopods were further subdivided into brachiopod spines, brachiopods and the pseudopunctuate brachiopod shells, whilst bryozoans were subdivided between encrusting and fenestral types. Fossil grains that could not be identified due to fragmentation were noted as unidentified fossil grains. Non-fossil components such as micrite, calcite cement, and quartz were also registered. Four hundred points were counted in each thin section to ensure the representation of smaller grains. Illustrated thin sections (Figs. 13 & 14) can be found in the palaeontological collections at the Natural History Museum, University of Oslo. They are numbered with the prefix PMO (referring to the former Palaeontological Museum in Oslo) followed by three letters indicating from which logged section the sample was collected (ALF – Alfredfjellet, HAM – Hambergfjellet, YMR – Ymerdalen, etc.). In each section, samples were collected from base to top and marked in a continuous fashion independent of actual stratigraphic level. Thus, as an example, PMO_HAM 1.10, refers to the thin section number 10 in the HAM1 section. For stratigraphic position of the thin sections, see Fig. 6.

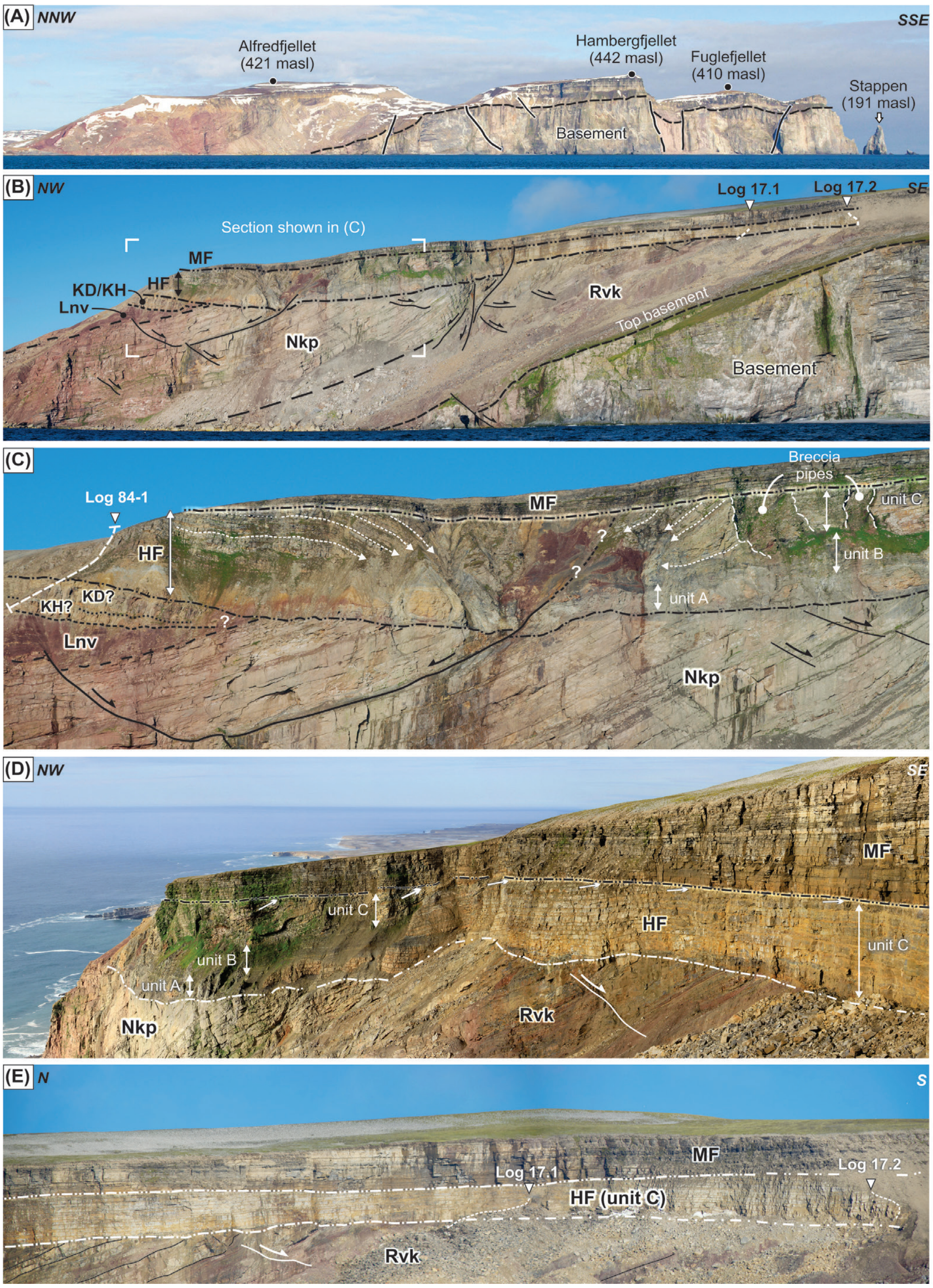

Figure 5. (A) Overview photo of the southwestern coastline of Bjørnøya. The stippled line indicates the boundary between the Hecla Hoek basement and the overlying upper Palaeozoic sedimentary succession. Note the presence of several faults (solid lines). (B) Photo of the stratigraphy exposed in the western to southwestern coastal cliff of Alfredfjellet. Note the lateral thinning of the Hambergfjellet Formation (marked HF) to the SE. Positions of logs 17.1 and 17.2 are indicated. The following abbreviations are valid for the remainder of the figures. Rvk – Røedvika Formation, Nkp – Nordkapp Formation, Lnv – Landnøringsvika Formation, KD – Kapp Dunér Formation, KH – Kapp Hanna Formation, HF – Hambergfjellet Formation, MF – Miseryfjellet Formation. (C) Close-up section of Alfredfjellet showing the threefold development of the Hambergfjellet Formation at this location. Note the varying dips (indicated by stippled white arrows) and breccia pipes in the upper unit, as well as a fault affecting both the Hambergfjellet Formation and the underlying units. Position of log 84-1 is indicated. (D) View north along the western side of Alfredfjellet. From this position the three-folded development is more obvious. Note the changing dip within the upper unit and the unconformable contact to both the underlying and overlying formations. (E) Photo illustrating the tabular, sheet-like geometry of unit C and the angular unconformities defining the top and base of the Hambergfjellet Formation. Note the low-angle character of the upper unconformity at this location (Alfredfjellet).

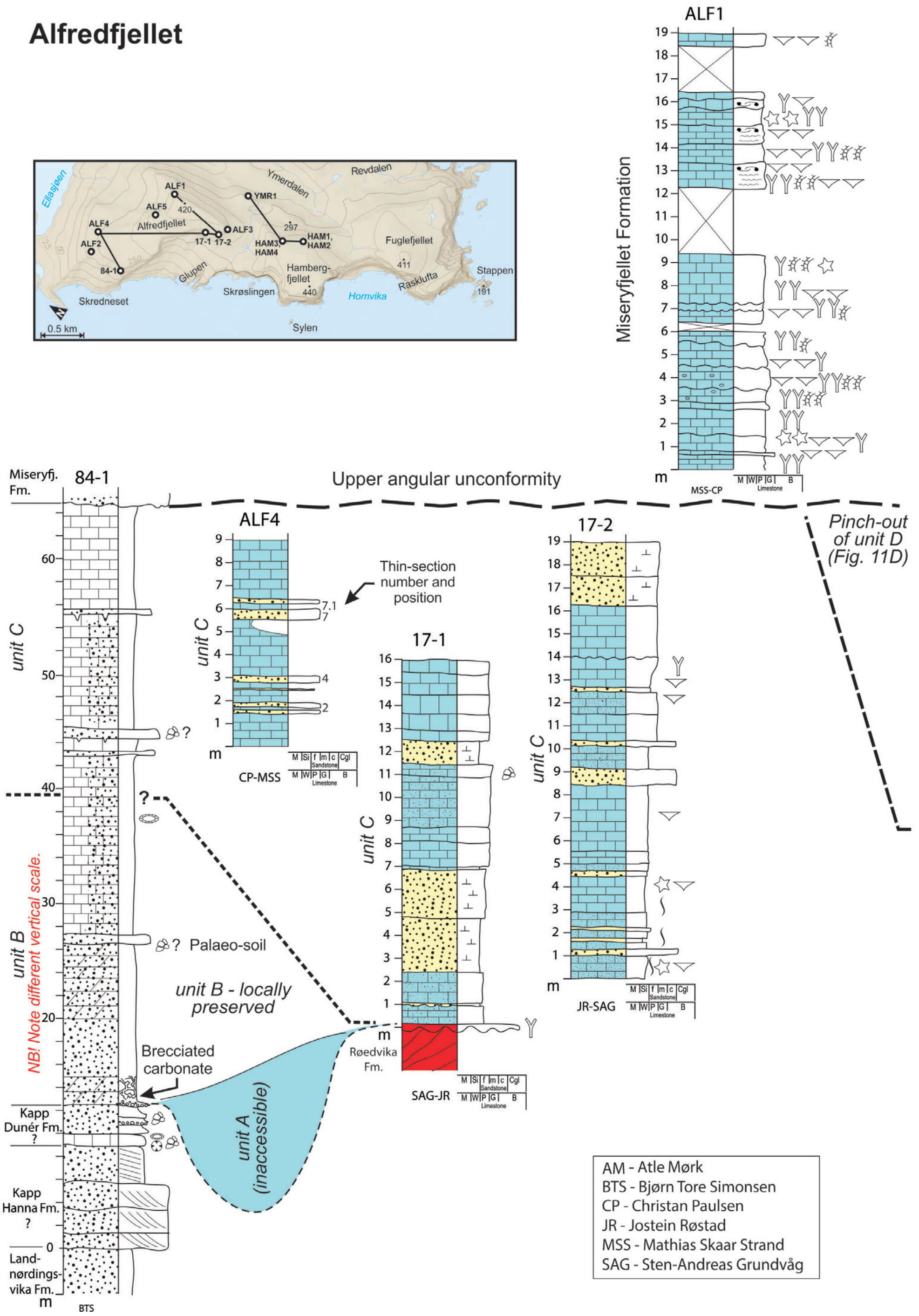
Alfredfjellet
ALF1
Miseryfjellet Formation
Upper angular unconformity
Pinch-out of unit D (Fig. 11D)
84-1
Miseryfj. Fm.
ALF4
17-2
17-1
Thin-section number and position
unit C
unit B
NB! Note different vertical scale.
Palaeo-soil
unit B - locally preserved
Brecciated carbonate
unit A (inaccessible)
Kapp Dunér Fm.
Kapp Hanna Fm.
Landnørdingsvika Fm.
Røedvika Fm.
CP-MSS
SAG-JR
JR-SAG
MSS-CP
BTS
AM - Atle Mørk
BTS - Bjørn Tore Simonsen
CP - Christan Paulsen
JR - Jostein Røstad
MSS - Mathias Skaar Strand
SAG - Sten-Andreas Grundvåg
Revdalen
Ymerdalen
Fuglefjellet
Hamberg-fjellet
Skrøslingen
Hornvika
Rasklufta
Stappen
Sylen
Skredneset
Glupen
Alfredfjellet
Ellasjøen
0.5 km

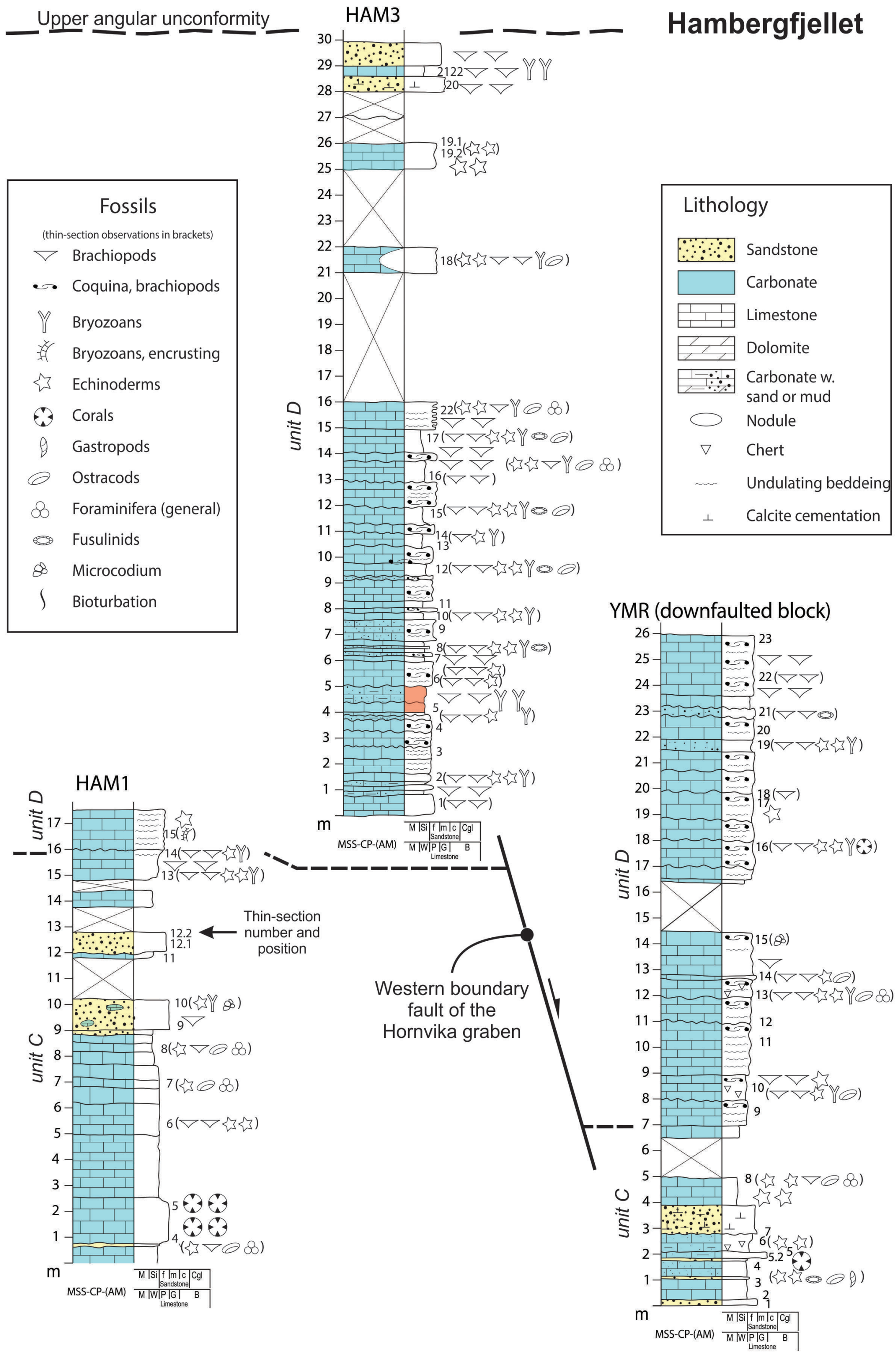

Figure 6. Panels showing the measured sections of the Hambergfjellet Formation at Alfredfjellet (left-hand side) and Hambergfjellet (right-hand side). The sections are shown in relative position to each other and have not been correlated one-to-one, nor have the panels been corrected for structural dip. Internal units and major surfaces are annotated. Note that log 84-1 has a different vertical scale than the other sections. Thin sections and their positions are indicated in each log.

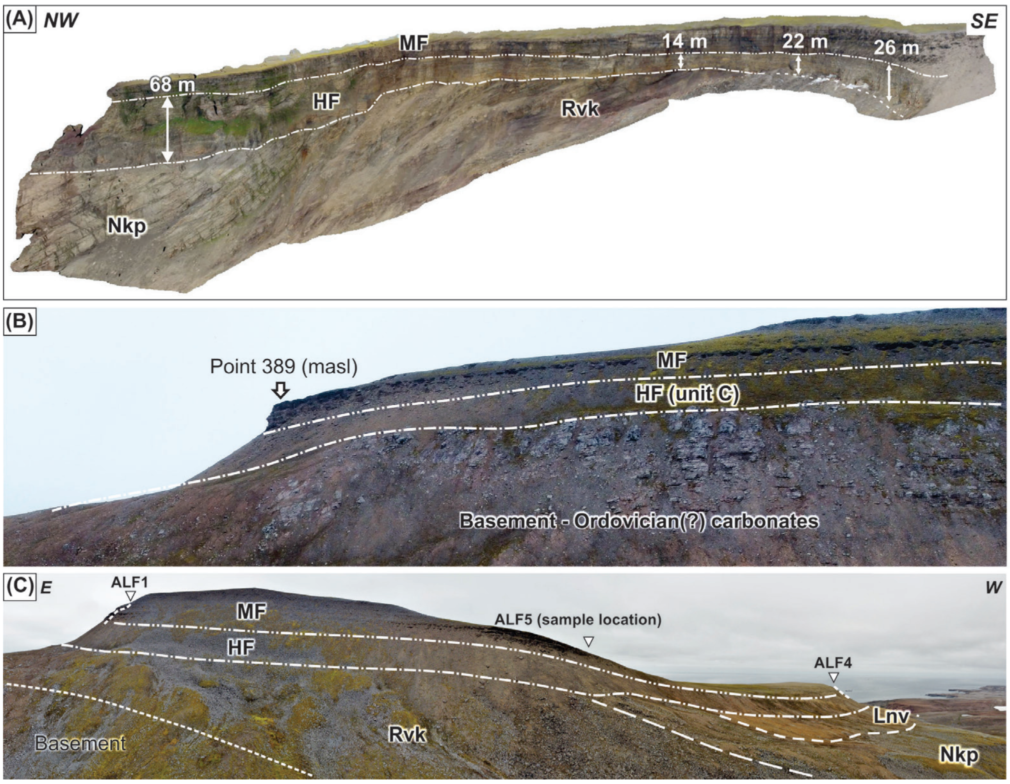

Figure 7. (A) Annotated digital outcrop model of the western side of Alfredfjellet with marked thickness measurements which demonstrate that the Hambergfjellet Formation thins significantly across the outcrop from c. 68 m to <14 m. (B) Photo demonstrating that unit C, while scree-covered, can be traced around from the western to the eastern side of Alfredfjellet as a thin sliver sandwiched between basement rocks and the Miseryfjellet Formation. (C) Photo showing the inferred position of stratigraphic boundaries and the investigated locations on the northern side of Alfredfjellet. A thin sliver of the Hambergfjellet Formation, presumably unit C, occurs between the Miseryfjellet Formation and the various older strata. Rvk – Røedvika Formation, Nkp – Nordkapp Formation, Lnv – Landnøringsvika Formation, KD – Kapp Dunér Formation, KH – Kapp Hanna Formation, HF – Hambergfjellet Formation, MF – Miseryfjellet Formation.

Results

Stratigraphic observations

The Alfredfjellet outcrop sections

At the south–west-facing aspect of Alfredfjellet, the Hambergfjellet Formation is conspicuously bounded below and above by angular unconformities (Figs. 5, 7 & 8; Horn & Orvin, 1928; Worsley et al., 2001). The erosive relief of the basal unconformity increases NW towards Skredneset in concert with a pronounced thickening of the Hambergfjellet Formation from *c*. 14 m to c. 68 m (Fig. 7A). In the cliff above Skredneset, the basal unconformity truncates a thin wedge-shaped sliver of upper Carboniferous sandstones and lower Permian carbonate rocks presumably belonging to the Kapp Hanna (late Moscovian–?Kasimovian Age) and Kapp Dunér (middle Gzhelian–late Asselian Age) formations, respectively (see log 84-1, Figs. 5C & 6). These deposits, in turn, appear to dip rather steeply to the east/northeast, thereby truncating the underlying redbeds of the Landnøringsvika Formation (Serpukhovian–Bashkirian) before terminating abruptly against the steeply-dipping top surface of the Upper Devonian–lower Carboniferous (Mississippian) Billefjorden Group. Furthermore, the basal unconformity of the Hambergfjellet Formation oversteps successively older strata to the SE including steeply dipping sandstones of the Billefjorden Group (Worsley et al., 2001; Figs. 5B, C & 8A). The upper angular unconformity at the base of the Miseryfjellet Formation truncates the Hambergfjellet Formation at a low angle (Figs. 5D, E & 8B).

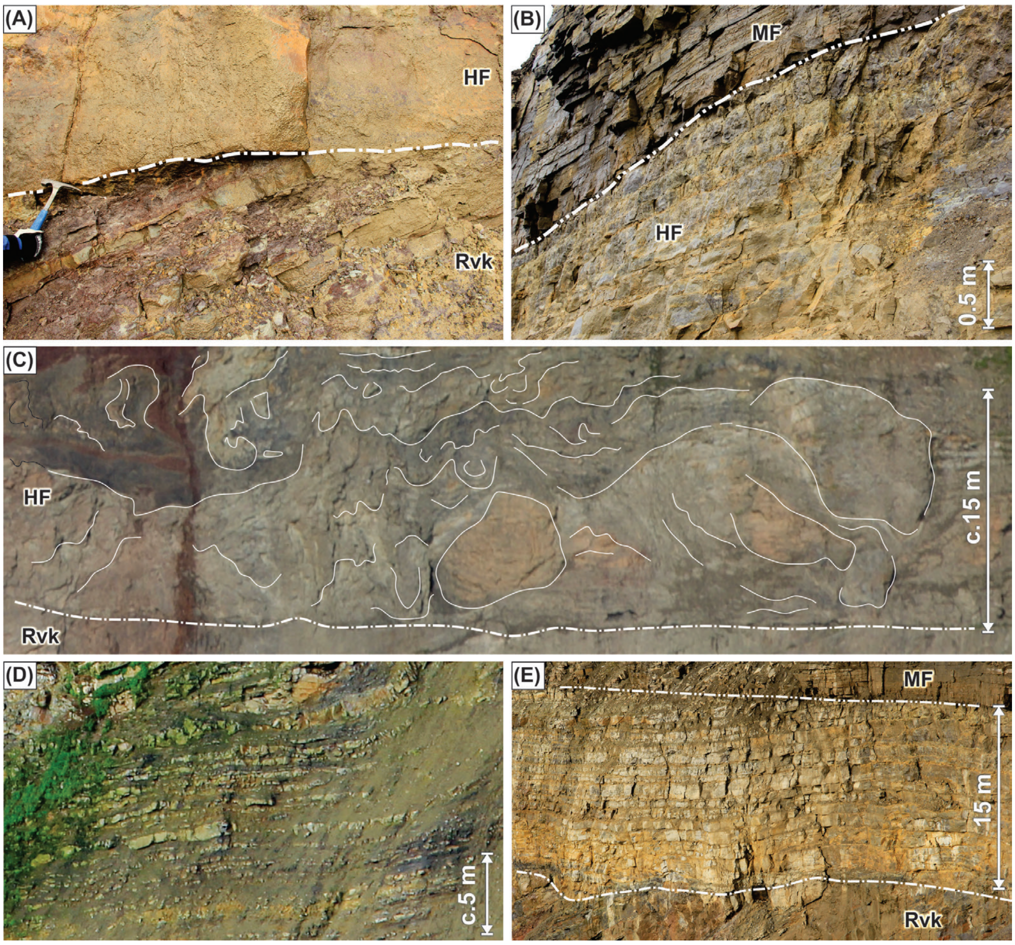

Figure 8. (A) In section 17-1 (see Fig. 6 for sedimentary log) on the western side of Alfredfjellet, unit C exhibit a sandstone-rich lower part and sits on the Røedvika Formation with an erosive and angular unconformity. (B) Photo showing the low-angle unconformity on top of unit C, which defines the basal surface of the overlying Miseryfjellet Formation. (C) Close-up photo showing the deformed and slumped character of unit A on the western side of Alfredfjellet. The unit is inaccessible and have only been investigated through binoculars and photographs. The unit appears to consist of variably sized carbonate slump blocks embedded in a mudstone rich matrix. (D) Photo illustrating the heterolithic and fine-grained character of unit B on the western side of Alfredfjellet. Section 84-1 document the facies of unit B and indicate mostly fine-grained dolostones void of fossils. (E) Photo from the western side of Alfredfjellet illustrating the well-developed bedding typical of unit C. The unit generally show a laterally constant thickness. Rvk – Røedvika Formation, HF – Hambergfjellet Formation, MF – Miseryfjellet Formation.

The Hambergfjellet Formation exhibits a threefold architecture at Alfredfjellet (Figs. 5D, E & 8). A *lower* chaotically-bedded to slump-folded unit (Fig. 8C), a *middle*, partly covered, heterolithic unit (Fig. 8D), and an *upper* carbonate unit exhibiting well-developed bedding can be recognized (Figs. 5C & 8E). In the remaining parts of the paper, these are informally referred to as *units A, B* and *C*, respectively.

Units A and B only occur in the thickest part of the formation and pinches out to the SE, whereas unit C have a sheet-like distribution across the entire cliff face (Fig. 5). Unit A is not accessible in any parts of the outcrop. From a distance, it exhibits a distorted and chaotically-bedded character and seemingly includes transported blocks of older, consolidated sedimentary rocks (Fig. 5C). Based on this appearance, we interpret these deposits to be slumped carbonate blocks embedded in dark-coloured mudstone. The 84-1 log spans units B and C (Figs. 5C & 6). The section includes a basal conglomerate succeeded by a 3 m-thick interval of brecciated dolostones, and a several tens of meters-thick succession of sand-rich, fossil-free, micritic limestones and rare interbedded sandstones. Palaeo-soil profiles, karst horizons, and in situ *Microcodium* occur at multiple levels (Fig. 6; Simonsen, 1991).

Unit C was investigated in two accessible sections at the south-western slope of Alfredfjellet (logs 17-1 and 17-2; Fig. 6), where its basal boundary is marked by a carbonate-rich conglomerate or carbonate-cemented sandstones capping the underlying steeply dipping strata of the Billefjorden Group (Figs. 5E & 8A). The remaining part of unit C consists of limestones with echinoderms, bryozoans, scattered brachiopods, and various trace fossils as well as subordinate sandstone interbeds (log 17-2; Fig. 6). Horizons bisected by complex fracture networks filled by sandstone and siltstone exhibiting a yellowish to reddish weathering colour are common, and well-developed (in situ) *Microcodium* was also recognized.

Internally, the dip of unit C becomes steeper to the NW and display opposing dips at each side of a normal fault SE of Skredneset. The fault, informally referred to as the *Alfredfjellet fault*, also affects the underlying lower Carboniferous Nordkapp Formation and defines a low-relief graben structure (Fig. 5B, C). Near the Alfredfjellet fault, unit C is bisected by several 20–30 m wide breccia pipes (Fig. 5C). These features have not been reported earlier and contradict previous investigations which indicate that karstification did not influence the Hambergfjellet Formation (cf., Stemmerik et al., 1999). The overlying Miseryfjellet Formation is not affected by either faulting or brecciation.

On the eastern slopes of Alfredfjellet, no outcrops of the Hambergfjellet Formation are seen to penetrate the scree-covered slope. Only pre-Devonian basement rocks crop out in the lower slope and Ordovician(?) limestones/dolostones occur in the southeastern slopes (Fig. 7B, C). However, from the geometric and stratigraphic relationships deduced on the western side of Alfredfjellet (Figs. 5, & 7A), it seems likely that unit C continues as a thin (<15 m) sliver sandwiched between the basement and the Miseryfjellet Formation, although buried beneath a thick scree cover (Fig. 7B, C). Fossil-free limestones with a reddish stain and a crystalline to fractured appearance, presumably belonging to unit C, occur in scattered outcrops on the northern slope of Alfredfjellet (locations ALF2 and ALF4; Fig. 1). The silicified, bryozoan packstones of the Miseryfjellet Formation and its basal conglomerate occur some few meters above the limestones.

The Hambergfjellet and Fuglefjellet outcrop sections

The coastal cliffs of Hambergfjellet and Fuglefjellet were studied from the seashore by boat and by tracing stratigraphic units on high-resolution photo mosaics (Figs. 9 & 10). The same threefold stratigraphic development is recognized with unit A only being locally preserved, the heterolithic unit B being partly vegetation-covered, and unit C displaying well-developed horizontal bedding (Figs. 9 & 10). A series of normal faults variably offset the top surface of the basement, and form several small, fault-bounded basins along the Hambergfjellet–Fuglefjellet transect (Figs. 9 & 10A). This gives rise to pronounced lateral thickness variations for the Hambergfjellet Formation across this part of the out-crop belt. Unit A is generally not affected by the faulting but is confined to the basins onlapping the Ordovician basement carbonate rocks (Fig. 9B). Unit B is present across the entire outcrop belt, albeit thinning across the crest of the fault blocks, or, where unit C erosively truncates the crest of the blocks, unit B is missing.

Previous stratigraphic observations of the seaside cliffs north–northeast of Hornvika (at the south to southeastern face of Hambergfjellet), suggest that the Hambergfjellet Formation caps yet another remnant of the Kapp Hanna and Kapp Dunér formations, which sits in a small graben structure (here referred to as the *Hornvika graben*) (Worsley et al., 2001, their figure 4). However, based on high-resolution photomosaics it is suggested here that the intra-graben strata should be assigned to the Upper Devonian Røedvika Formation (Fig. 9C, D). Evidence includes a characteristic red weathering colour (typical of the Røedvika Formation elsewhere on the island), the heterolithic nature of the sediments, and the presence of lenticular sandstone units exhibiting crossbedding.

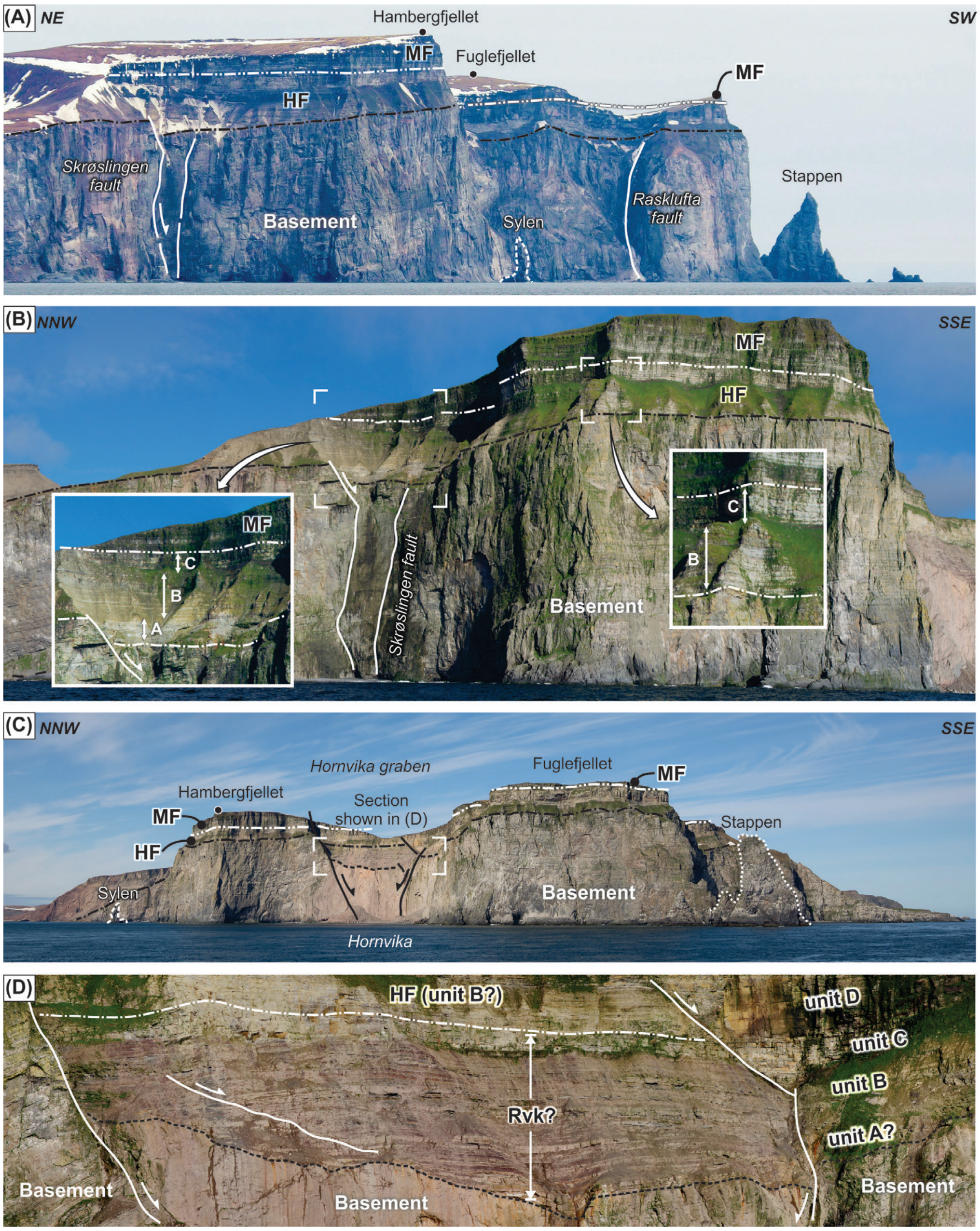

Figure 9. (A) Overview of the northwestern faces of Hambergfjellet and Fuglefjellet. Note the thickness variation of the Hambergfjellet Formation near the Skrøslingen fault. (B) Photo of the northwestern to southwestern seaside cliff of Hambergfjellet north of Hornvika. At this location, the Hambergfjellet Formation onlaps a basement high consisting of Ordovician limestones/dolostones of the Ymerdalen Formation. The Hambergfjellet Formation is thickest near the Skrøslingen fault where units A to C is present (left inset). Unit A is not present over the crest of the rotated basement block (right inset). (C) View NE towards Hornvika and the southwestern faces of Hambergfjellet and Fuglefjellet. Here, two steeply dipping faults define the Hornvika graben. (D) The eastern boundary fault of the Hornvika graben juxtaposes the Hambergfjellet Formation against strata inferred to be of the Røedvika Formation. Note the occurrence of unit D in the upper right corner. This unit is best developed in the outcrops east of the western boundary fault. Rvk – Røedvika Formation, HF – Hambergfjellet Formation, MF – Miseryfjellet Formation.

The faults defining the Hornvika graben offset both the Hambergfjellet and Miseryfjellet formations (Fig. 9). On Fuglefjellet on the eastern side of the Hornvika graben, a peculiar, sharp-based, c. 25–30 meters thick unit with a massive lower part and a thin-bedded upper part visibly caps unit C (Fig. 10B). The unit can be traced west across the western boundary fault of the graben where it thins and disappears abruptly underneath the low-angle unconformity at the base of the Miseryfjellet Formation. As such, it appears to be a separate stratigraphic unit, which we refer to as *unit D*,

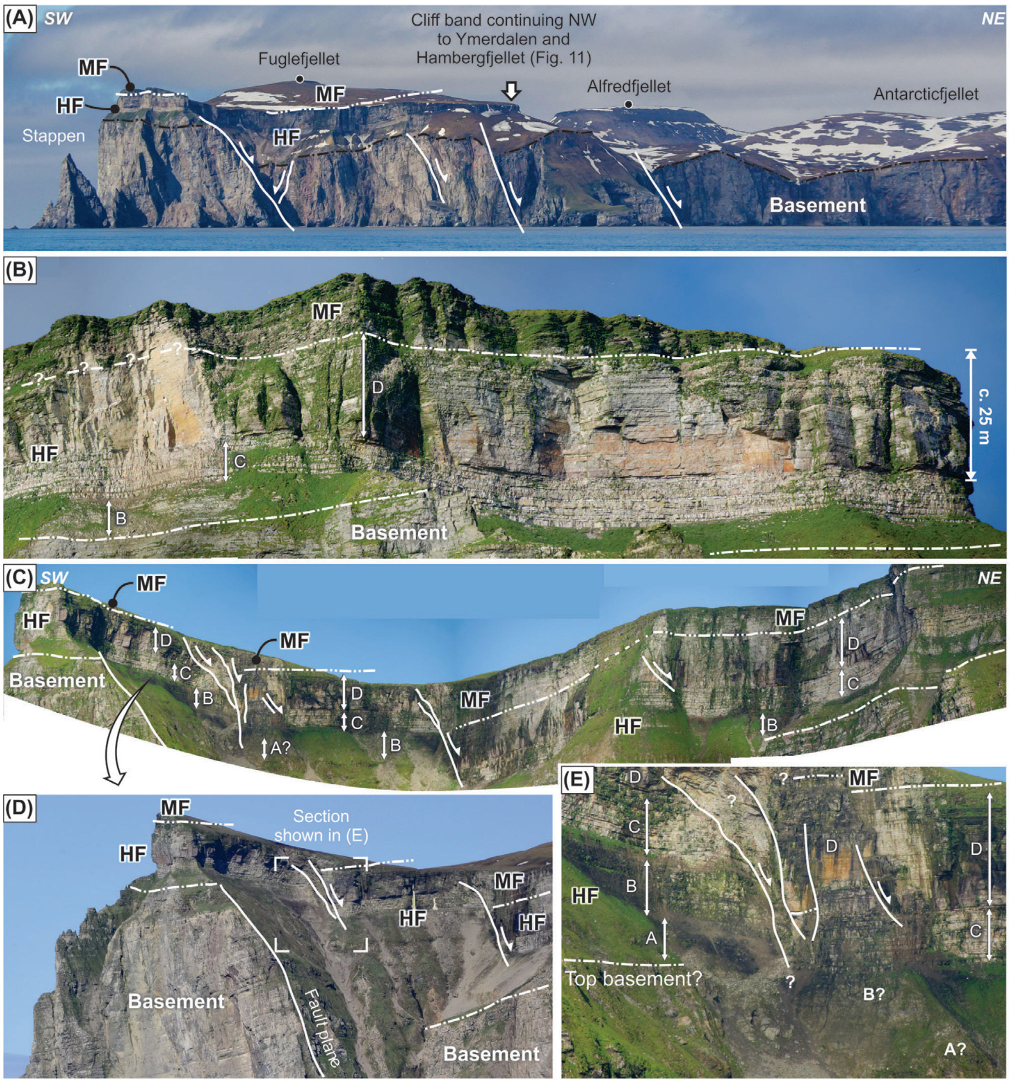

Figure 10. (A) Overview of the southeastern tip of Bjørnøya. Here, several faults transect the basement and defines a series of rotated fault blocks that appear to step down to the east–southeast. (B) Photo showing the threefold development of the Hambergfjellet Formation at the southern tip of Fuglefjellet. The well-developed bedding of unit C and the sharp base and thick-bedded character of unit D is clearly visible. (C) Some of the faults offset both the Hambergfjellet and Miseryfjellet formations possibly testifying to Mesozoic rifting in the area. Photo from the south-eastern face of Fuglefjellet. (D) Photo showing the lateral continuation of the Rasklufta fault plane on the south-eastern side of Fuglefjellet. Several smaller fault strands occur within the main fault zone and appear to transect both the Hambergfjellet and Miseryfjellet formations. (E) An attempt to trace the internal units of the Hambergfjellet Formation across one of the fault strands of the Rasklufta fault. Unit A is only present within the deepest parts of this fault-bounded basin. HF – Hambergfjellet Formation, MF – Miseryfjellet Formation.

implying an assignment to the Hambergfjellet Formation. As will be shown later, lateral tracing of this unit in combination with previously proposed ages for the Hambergfjellet Formations based on fusulinids provide support to our assignment.

On the south-eastern aspect of Fuglefjellet, a series of normal faults successively step down towards the east to SE, defining several fault-bounded basins (Fig. 10). Some of the faults affect the basement carbonate rocks, all the internal units of the Hambergfjellet Formation, and the Miseryfjellet Formation, thus making stratigraphic work challenging (Fig. 10A, C–E). However, because unit D is easily recognized in all the cliffs, it can be used as a marker horizon for structural reconstructions (Fig. 10C–E). Unit D appear to thicken slightly across the main faults. Whether this is stratigraphic thickening/growth controlled by the fault or whether it relates to increased preservation in the basin due to preferential erosion is uncertain. Locally, small faults with offsets less than a couple of meters are seen to affect unit D, rapidly soling out atop unit C.

Unit D protrudes the vegetation covered slope on the eastern and northeastern slopes of Fuglefjellet, forming a prominent cliff band which turns NW into Ymerdalen across to the eastern / northeastern slopes of Hambergfjellet (Fig. 11). Here, unit C was investigated in poorly exposed outcrops below the cliff-forming unit D (log HAM1; Figs. 6 & 11). Unit C consists of mudstone to wackestone containing varied fauna elements, including a pronounced two meters-thick bed containing abundant colonial rugose corals, as well as subordinate sandstone interbeds (Figs. 6 & 12A). Unit D is dominated by thick-bedded brachiopod grainstones, abundant echinoderms, thumb-sized bryozoans, fusulinids, and exhibit moderate silicification (see log HAM3, Figs. 6, 11 & 12B, C). Locally, a characteristic reddish colour is present (Fig. 12D). The bryozoan-dominated, brachiopod-rich packstones of the Miseryfjellet Formation forms another cliff band near the top of the Hambergfjellet plateau (Figs. 11C, D & 12E, F). Unit D thins markedly to the NNW (Fig. 11D). At first glance, this appreciable thinning may be

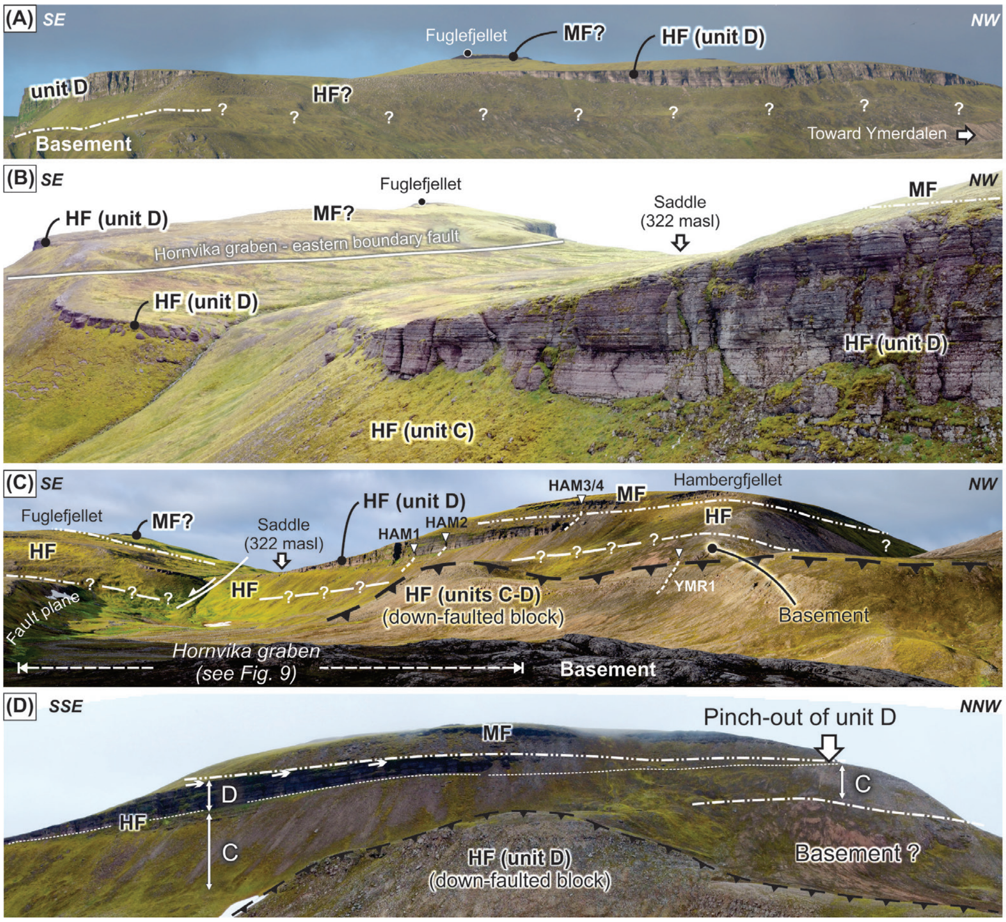

Figure 11. (A) Photo documenting the development of the Hambergfjellet Formation at the southeastern to northeastern faces of Fuglefjellet. Here, units B and C is generally vegetation covered, whereas unit D, which is partly silicified, forms a prominent cliff band that can be traced northwestward into Ymerdalen. (B) Unit D is accessible along the cliff band on the northwestern slopes of Hambergfjellet, whereas unit C is poorly exposed in the gentle slopes below the cliff. Based on data from this outcrop, Nakrem (1991a) assigned a late Artinskian age to the interval corresponding to our unit D. (C) Overview photo looking south from Ymerdalen showing the northeastern side of Hambergfjellet where units C and D is exposed. Sections HAM1 to HAM4 was measured on the prominent cliff band whereas the YMR1 section was measured on the down-faulted block. Note that the valley margins of Ymerdalen represent the northward continuation of the faults defining the Hornvika Graben (see Fig. 9). (D) Photo showing the angular unconformity between unit D and the overlying Miseryfjellet Formation, as well as the northwestward pinch-out of unit D on Hambergfjellet. Unit D is well preserved in the down-faulted block in Ymerdalen and in all outcrops east of the Hornvika graben, but do not occur west of its western boundary fault. HF – Hambergfjellet Formation, MF – Miseryfjellet Formation.

Figure 12. (A) Unit C contains a varied warm-water fauna including corals at multiple levels. The photo show parts of a densely packed coral layer in the lower part of the YMR1 section. (B) Photo showing a thick stack of brachiopod-dominated grainstone beds in unit D documented in log HAM3. (C) Thick-shelled and disarticulated brachiopods characterize unit D. (D) A reddish stained part of unit D (in section HAM3, see Fig. 6) containing thumb-sized fenestral bryozoans, crinoids and smaller sized brachiopods embedded in a reddish mudstone matrix (see thin-section photo in Fig. 14E). This feature is not seen elsewhere in the Hambergfjellet Formation. (E) Bryozoans of various types dominate the Miseryfjellet Formation, possibly reflecting deeper waters across the Stappen High during the late Permian. (F) Brachiopods are locally abundant in the Miseryfjellet Formation.

mistaken for an effect caused by diminishing outcrop quality and increasing vegetation cover. However, upon closer inspection, there is an angular unconformity between the southeast-dipping layers of unit D, and the overlying, horizontally-bedded Miseryfjellet Formation. Because unit D is not present on Alfredfjellet further to the north (Fig. 7), unit D must pinch out rather abruptly to the NW at <750 m (Fig. 11D). Furthermore, given the thick development on Fuglefjellet, Unit D seems to thicken substantially across the western boundary fault of the Hornvika graben, consistent with our observations from the coastal cliffs.

The Ymerdalen outcrop section

The YMR1 log (Figs. 6 & 11) is located on a down-faulted block on the western margin of Ymerdalen. While Horn & Orvin (1928) interpreted the outcrop to be a landslide derived from the eastern slopes of Hambergfjellet, Dallmann & Krasil'ščikov (1996) interpreted it as a result of tectonics as previously suggested by Holtedahl (1920), a view supported by our study. Two normal faults, one striking north–south and another NW–SE, has displaced the section down into Ymerdalen (Figs. 3B & 11). It is also suggested here that the faults which define the Hornvika graben in the coastal section between Hambergfjellet and Fuglefjellet (cf., Fig. 9C, D) continue northward into Ymerdalen, possibly linking up with the basement lineaments running parallel to the valley margins (Fig. 3B & 11B). Andersson (1899) and Holtedahl (1920) mapped coal-bearing sandstones of the Røedvika Formation in the innermost part of Ymerdalen. This local occurrence of Upper Devonian sandstones was removed from later maps by Horn & Orvin (1928) who did not find any such in situ exposures. Instead, they suggested the presence of a landslide block containing lower Carboniferous sandstones. However, considering the possible occurrence of Røedvika Formation deposits of the Hornvika graben on the seashore (Fig. 11) and its proposed northward/landward continuation, this discrepancy needs to be investigated further for clarification.

Because of the complicated structural setting in Ymerdalen, there are some uncertainties in correlating the YMR1 section with the nearby in situ sections (Fig. 6). However, a silicified coral bed, mainly consisting of densely-packed colonial rugose corals, was used as a marker bed for a tentative correlation to the HAM1 section (Fig. 6). At approximately 7 m above the base, there is a marked transition from mudstones and wackestones into brachiopod-dominated beds rich in articulate brachiopods. It is suggested here that the YMR1 section covers the uppermost few meters of unit C, whereas the transition into brachiopod-dominated beds marks the base of unit D. The stratigraphic development is thus very similar to that documented in the combined HAM1 and HAM3 sections measured on the slopes above Ymerdalen (Figs. 6 & 11). The Hambergfjellet Formation wedges out north-eastward and is completely absent both at Antarcticfjellet on the eastern side of Ymerdalen, as well as at Miseryfjellet further to the NE.

Facies and microfacies analysis

The Hambergfjellet Formation consists of mixed carbonate and siliciclastic rocks. Based on field observations (Figs. 6 & 12) and thin-section analysis, we recognize five principle sedimentary facies (Figs. 13 & 14). We name them according to the most common grain types, grain size, or other lithological characteristics. In addition, diagenetic overprinting of the carbonate facies caused by subaerial exposure are recognized in some horizons. As such, we describe *Microcodium* separately. The thin-section analysis reveals two main populations in terms of composition and fossil contents, where the first is attributed to unit C and the second to unit D (Fig. 15). No samples are available from units A and B due to inaccessible outcrops. In thin sections, unit C is characterized by a low-content, low-diversity fossil fauna, though with most grains altered into micrite (Figs. 13 & 15). Unit D exhibits a clear increase in the abundance of fossil fragments whereby brachiopods and echinoderms dominate over subordinate amounts of bryozoans (Figs. 14 & 15). In outcrop, the Miseryfjellet Formation is evidently rich in bryozoans. However, in the few analysed thin sections, echinoderms and brachiopods are dominant. A description of the recognized microfacies is given below.

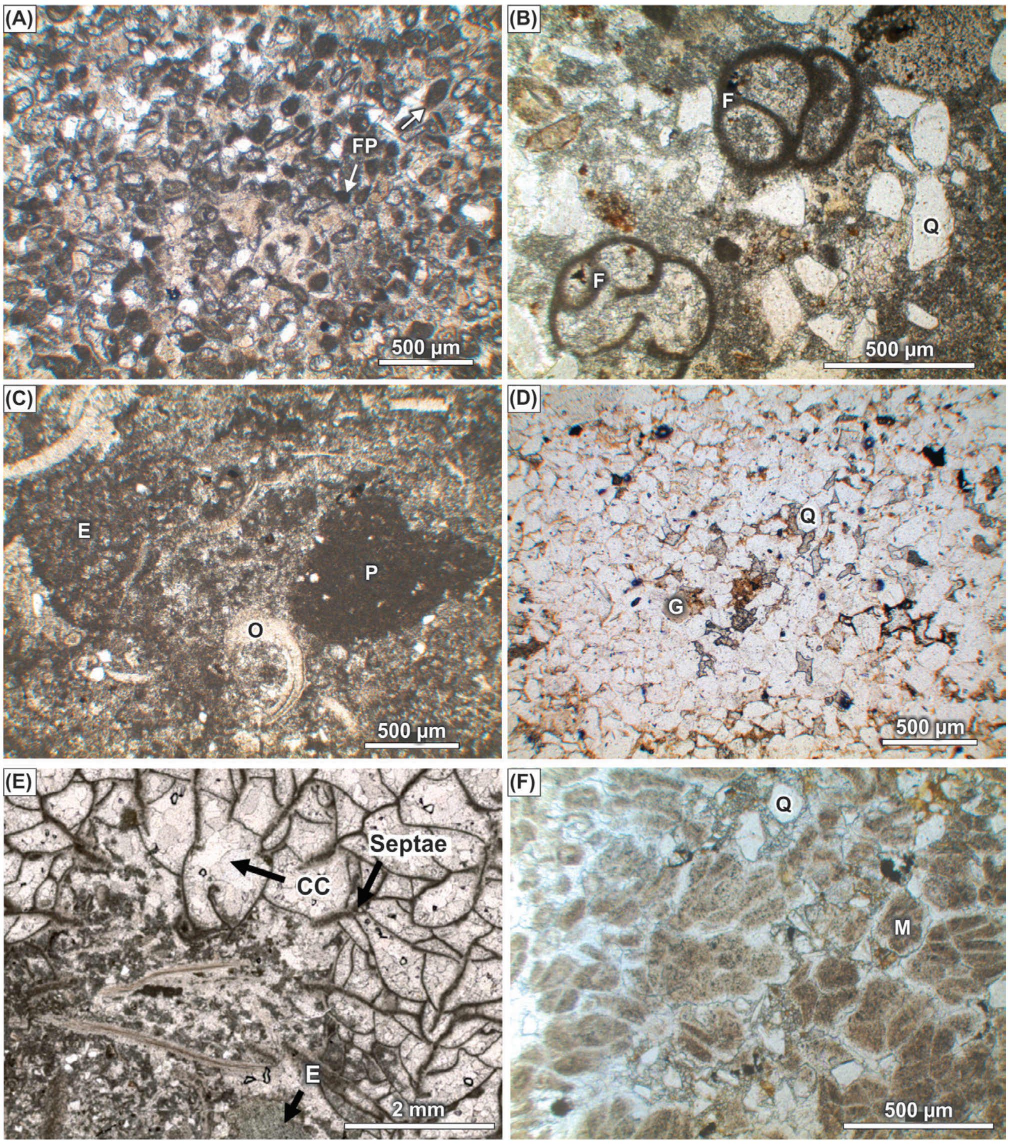

Figure 13. Thin-section photomicrographs from unit C of the Hambergfjellet Formation. All thin sections are shown in plane-polarized light. (A) Wackestone consisting of oval micrite pelliods of faecal pellets. Sample PMO_HAM 1.6. (B) Wackestone containing micritised foraminifera (F) *and quartz grains* (Q)*. Sample PMO_HAM 1.3. (C) Wackestone with ostracod shells* (O)*, echinoderms* (E)*, and pelloids* (P) *in a micritic matrix. Sample PMO_YMR 1.8. (D) Mature, quartz-rich sandstone with subordinate grains of glauconite and variable amounts of calcite and silica cement. Sample PMO_YMR 1.22. (E) Coral facies where calcite cement in the size of sparite* (CC) *occur between the individual coral-septae. Micrite and benthic fossil components such as echinoderms* (E) *are also present. Sample PMO_HAM 1.4. (F) Microcodium aggregates* (M) *co-occurring with subordinate quartz grains* (Q)*. Sample PMO_YMR 1.15. See Fig. 6 for stratigraphic position of the samples/thin sections.*

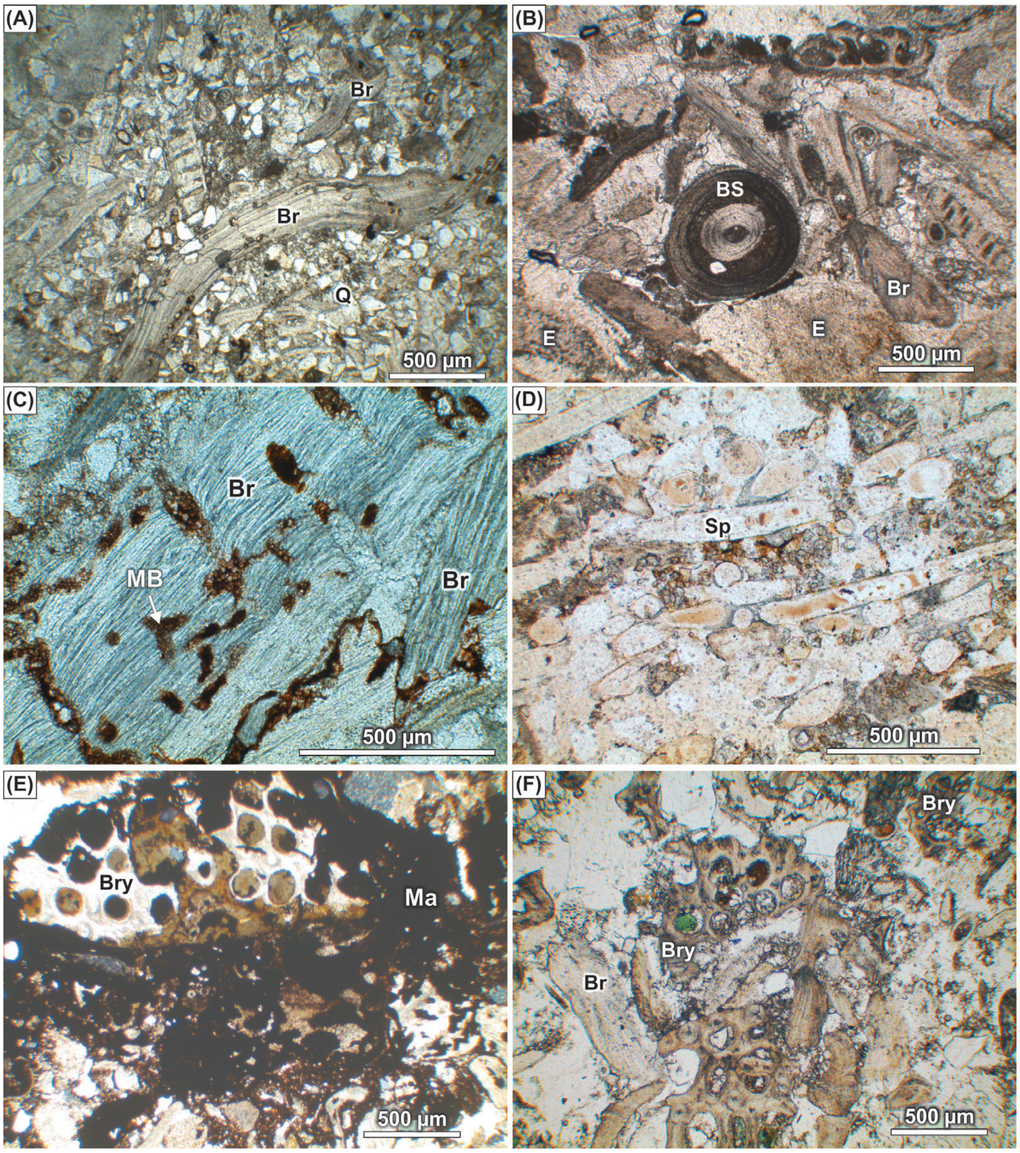

Figure 14. Thin-section photomicrographs from unit D of the Hambergfjellet Formation and the lowermost part of the Miseryfjellet Formation. All thin sections are shown in plane-polarized light. (A) Sandstone-rich brachiopod grainstone to packstone containing abundant brachiopod fragments (Br) *and quartz grains* (Q). *Sample PMO_HAM 3.8. (B) Brachiopod* (Br) *grainstone with micrite filling in pores. Micrite-filled brachiopod spine* (BS), *as well as echinoderm grains* (E) *are frequently present. Sample PMO_YMR 1.13. (C) Many brachiopod shells* (Br) *exhibit Trypanites micro-borings* (MB). *Sample PMO_HAM 3.3. (D) Unit D is extensively silicified in comparison to the underlying units. Here, the photo shows silicified sponge spicules* (Sp). *Sample PMO_HAM 3.18. (E) Sample illustrating the appearance of the reddish-stained interval in unit D in the HAM3 section. This interval is rich in bryozoans* (Bry) *embedded in a fine-grained, red-colored matrix* (Ma). *Sample PMO_HAM 3.5. (F) The Miseryfjellet Formation is characterized by packstones dominated by bryozoans* (Bry) *and subordinate brachiopods* (Br). *Sample PMO_HAM 3.22. See Fig. 6 for stratigraphic position of the samples/thin sections.*

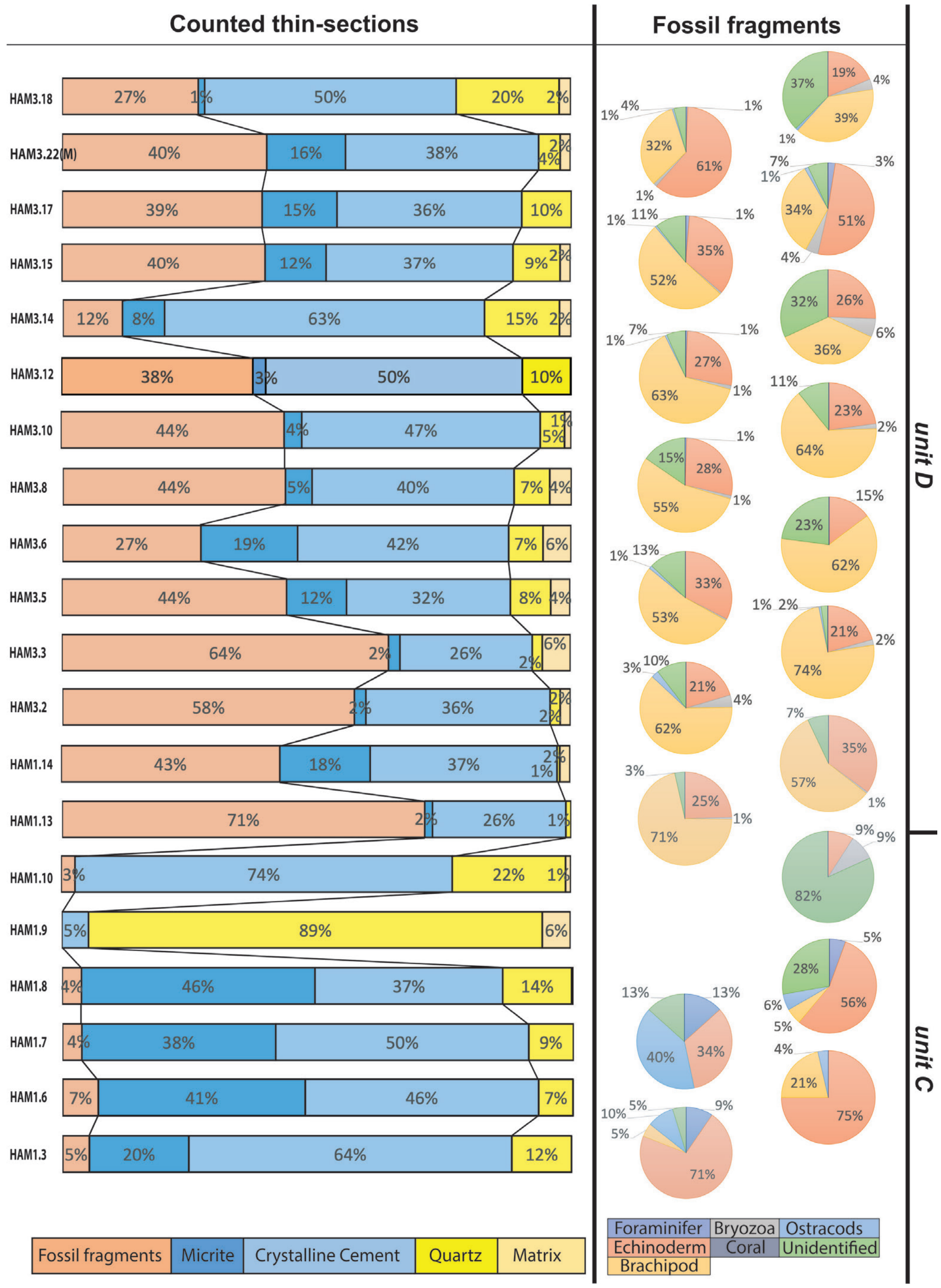

Figure 15. Counted thin sections from samples collected in the HAM1 and HAM3 logs. Samples PMO_HAM 1.3 to PMO_HAM 1.10 document the high abundance of micrite in unit C. The low abundance of fossils and extensive micritization makes it difficult to identify fossil grains. A quartz-rich, calcite cemented sandstone without any fossil grains are seen in sample PMO_HAM1.9. Samples PMO_HAM 1.13 to PMO_HAM 3.18 document the composition of unit D. Note the dominance of brachiopod grains. Sample positions are marked in the HAM1 and HAM3 logs (Fig. 6).

Mudstone/wackestone facies

Description. – Micrite-rich carbonate mudstones commonly grading into wackestones were identified from the field and verified by the microfacies study. There is a low presence of fossil fragments (Fig. 13). Benthic foraminifera and other micritized invertebrate fossils are variably present, including echinoderms, subordinate brachiopods, corals, and ostracods, which occasionally form chaotically organized skeletal grain accumulations (Fig. 13A–C). Faecal pellets are abundant as well as pelloids and minor amounts of quartz grains (Fig. 13A). Angular lithoclasts are variably present.

Interpretation. – Micrite and the allomicritic destruction of invertebrate grains indicate deposition in shallow marine environments within the photic zone (Flügel, 2004). Faecal pellets are commonly preserved in subtidal, lower-intertidal zones of inner ramps or platform setting (Flügel, 2004). Faecal pellets are relatively soft and intragranular cement is formed in warm-water settings like the present-day interior of the Bahamian Platform (Wanless et al., 1981). Chaotically organized skeletal grains imply some energy during deposition. The quartz grains and lithoclasts may be the result of in situ mixing and terrigenous supply, whereas the angular clast shapes point to short transportation distances. The presence of calcite cement implies eogenetic diagenesis (Bathurst, 1971). This facies is therefore interpreted to be a shallow marine deposit which accumulated in an inner platform environment.

Sandstone facies

Description. – Sandstones are variably interbedded with the limestones of unit C and unit D (e.g., in the 17-1, 17-2, HAM1, YMR1, ALF4 sections; Figs. 6, 8A & 13D). Thick sandstone beds occur in particular in the lower part of unit C, which locally truncates sandstone-dominated strata of the Billefjorden Group (Fig. 8A). Siliciclastic grains also occur scattered in the limestone samples in all the logged sections, for example ranging from 1% to 20% (averaging 9%) of the solids in the HAM1 and HAM3 profiles (Fig. 15). Glauconite occurs locally in the sandstones of unit D (in the YMR1 and HAM3 sections, e.g., Fig. 13D). Petrographic analysis of sandstone beds shows quartz-rich, moderately sorted, very fine- to fine- and medium-grained compositions with subangular to subrounded grains. Chert grains and traces of mica are present in all samples, feldspar is rare, and rutile, zircon, and tourmaline occur as accessory stable heavy minerals. The sandstone compositions range from strongly quartz-cemented and compacted quartz arenite (thin sections PMO_HAM 1.9.1, PMO_HAM 1.9, PMO_ALF 4.7; see Fig. 6 for stratigraphic position) with only minor interstitial carbonate cement, to strongly carbonate-cemented quartz-rich sandstone with carbonate peloids (thin sections PMO_HAM 1.10, PMO_HAM 1.12.2, PMO_YMR 1.7; see Fig. 6 for stratigraphic position), and scattered siliciclastic grains enclosed by poikilotopic carbonate cement (thin section PMO_ALF 4.4). Carbonate pelloids are outlined by rusty rims and inclusions in strongly cemented samples.

Interpretation. – The sandstone content indicate proximity to exposed land which acted as a source for siliciclastic material, and the thick occurrences in the base of unit C indicates transgressive reworking of exposed sandstone-bearing terrane. The rounded zircons and tourmaline indicate sedimentary recycling of older sandstone strata. Textural evidence includes replacement of feldspar by carbonate cement, suggesting diagenetic impacts on the mineralogical maturity (thin sections PMO_HAM 1.12.1, PMO_ALF 4.7). The carbonate-dominated sandstones (≥2 / 3 allochem + cement) suggest an origin as quartz-rich packstones and wackestones, deposited in environments of mixed carbonate-siliciclastic sedimentation. Quartz cementation occurring as overgrowths on detrital quartz grains is pronounced in the few studied sandstone samples characterized by low total carbonate contents. Chemical compaction by close grain packing and quartz cementation as in thin section PMO_HAM 1.9 suggest extensive burial diagenesis. Notably, quartz cement is absent where quartz grains are isolated within carbonate cement. Carbonate cementation has occurred in distinct stages, predating and postdating quartz cementation. The last phase is responsible for extensive replacement of labile grains as evidenced by oxidised coatings and traces of detritial grains within the carbonate cement. Burial diagenetic quartz cementation is temperature-dependent and common in quartz-rich sandstones from 80°C to 175°C (e.g., Walderhaug, 1994). The extensive quartz cementation of local quartz sandstone beds in the Hambergfjellet Formation can be explained by palaeotemperatures previously modelled in the range of 150–160°C during the Mesozoic subsidence of Bjørnøya (Ritter et al., 1996; Worsley et al., 2001). However, Nakrem (1991a), derived lower temperatures based on conodont Color Alteration Index values of 1.5–2, which correspond to burial temperatures of 50–140°C.

Coral packstone/grainstone facies

Description. – Coral-bearing packstones to grainstones were identified in the field forming laterally persistent beds. Both rugose colonial and tabulate corals were recognized (Figs. 12A & 13E). Most corals have an infill of sparite, and silica have locally replaced both the sparite and the coral structure (Fig. 13E).

Interpretation. – The various corals identified here are typical corals of the late Palaeozoic with both tabulate and colonial rugose corals. These corals are facies indicators of warm, shallow marine, nutrient-rich environments, whereas the orientation of the individual coral colonies implies an energy-rich environment with post-mortem reworking (Flügel, 2004).

Microcodium overprinted carbonates

Description. – Well-developed, in situ *Microcodium* are present in the carbonates (i.e., within the mudstone/wackestone and packstone/grainstone facies) of unit C at Alfredfjellet (log 17-1; Fig. 6), and as disarticulated grains in several thin sections from both units C and D (logs HAM1 and YMR1; Figs. 6 & 13F). In the thin sections, *Microcodium* is present as brownish/yellowish grains with blade-like structure and undulating extinction often radiating from a centre (Fig. 13F).

Interpretation. – *Microcodium* is commonly found in the upper Carboniferous to lower Permian succession of Svalbard, and in situ varieties have traditionally been used to identify palaeo-soils formed during subaerial exposure under arid climates (Kabanov et al., 2008; Blomeier et al., 2011; Ahlborn & Stemmerik, 2015). However, erosion of palaeo-soils may also result in transport and redeposition of *Microcodium* grains. Thus, in the Hambergfjellet Formation, where both varieties exist, the in situ horizon implies subaerial exposure of the carbonate platform, whereas the scattered occurrence of disarticulated grains indicates reworking of older soils.

Bioclastic brachiopod packstone/grainstone facies

Description. – There is a prominent change from micrite and calcite-cemented sections in unit C transitioning into mostly packstone/grainstone consisting of brachiopods in unit D (Figs. 6 & 15). Brachiopod packstone/grainstone facies is characterized by a low presence of mud and a high abundance of brachiopods, echinoderms, and locally fusulinids. Heterogeneous mixtures of fossil sizes and fragmentation are seen in thin sections (Fig. 14A–D). The amount of quartz grains and silicification of the brachiopod fragments vary but tend to increase upwards in unit D. Micrite within grains are observed in places as well as bioturbation and microbial borings (Trypanites type, e.g., Uchman et al., 2016) of the brachiopod shells. In outcrop, some packstones exhibit a reddish weathering colour (Fig. 12D). In thin section, these packstones consists of crushed and fragmented grains of brachiopods, echinoderms and subordinate bryozoans embedded in a fine-grained reddish matrix (Fig. 14E).

Interpretation. – The crushed and fragmented fossils, partly infilled with micrite, but occurring as packstone to grainstone, suggest a shallow marine depositional environment of variable but generally high energy levels. Oxidation of either ferrous calcite or iron-bearing siliciclastic constituents precipitated hematite to produce the subsequent reddish matrix.

Bryozoan packstone facies

Description. – The Miseryfjellet Formation (documented in the uppermost part of logs HAM3 and ALF1; Fig. 6) is characterized by silicified packstones which have a higher abundance of bryozoans compared to units C and D of the Hambergfjellet Formation. Both fenestral and encrusting bryozoans with calcite infill were observed in thin section (Figs. 14F & 15). Some quartz grains are also present. Brachiopod grains, occurring both as pseudopunctuate and impunctuate, are variably present.

Interpretation. – While bryozoans are known from many warm-water carbonate platform successions (e.g., Nakrem, 1994), they are very common constituents of cool-water carbonate platforms. Bryozoans occur abundantly in various parts of the Bjarmeland and Tempelfjorden groups, where they occur as reef builders (Larssen et al., 2002). The marked increase of bryozoans in the Miseryfjellet Formation in comparison to the Hambergfjellet Formation, therefore, marks a transition into colder waters (Worsley et al., 2001). The same patterns of shifts to colder waters are also seen in other depositional basins along the northwestern margin of Pangaea (Beauchamp, 1994; Beauchamp & Desrochers, 1997; Stemmerik, 1997; Reid et al., 2007; Bensing et al., 2008). The encrusting bryozoan recognized in thin section is identified as the genus *Cyclotrypa* or *Fistulipora* known from both the Miseryfjellet and the Kapp Starostin formations (personal communication, H.A. Nakrem, Natural History Museum, University of Oslo).

A composite type section for the Hambergfjellet Formation

This study demonstrates that no single section can account for the complex lateral and stratigraphic development of the Hambergfjellet Formation (Fig. 6). Therefore, we propose a composite type section for the Hambergfjellet Formation (Fig. 16). The thickness of the composite section is based on estimated average thicknesses derived from the digital outcrop model and by extrapolating thicknesses from measured sections (Figs. 6 & 7A).

Unit A has a very localized occurrence and is restricted to the series of fault-bounded basins documented here, thereby exhibiting significant lateral thinning–thickening trends due to underlying fault-related topography. It has an average thickness of c. 15 m in the western face of Alfredfjellet, although it pinches out both to the NW and to the SE and locally thickens to *c*. 20 m. The unit has a possible maximum thickness of >30 m in some of the other fault-bound basins (e.g., in the southeastern part of Fuglefjellet near the Rasklufta fault; Figs. 9 & 10).

The thickness of unit B ranges from 0 m to 25 m, with an average of *c.* 20 m at Alfredfjellet. Unit B is generally present along most of the outcrop belt of the coastal cliffs, though it commonly thins significantly across the crest of some of the rotated basement fault blocks. Unit C is laterally extensive and displays a very consistent thickness with an estimated average thickness of *c.* 18 m. Both the minimum (14 m) and maximum (30 m) thicknesses are measured on the western side of

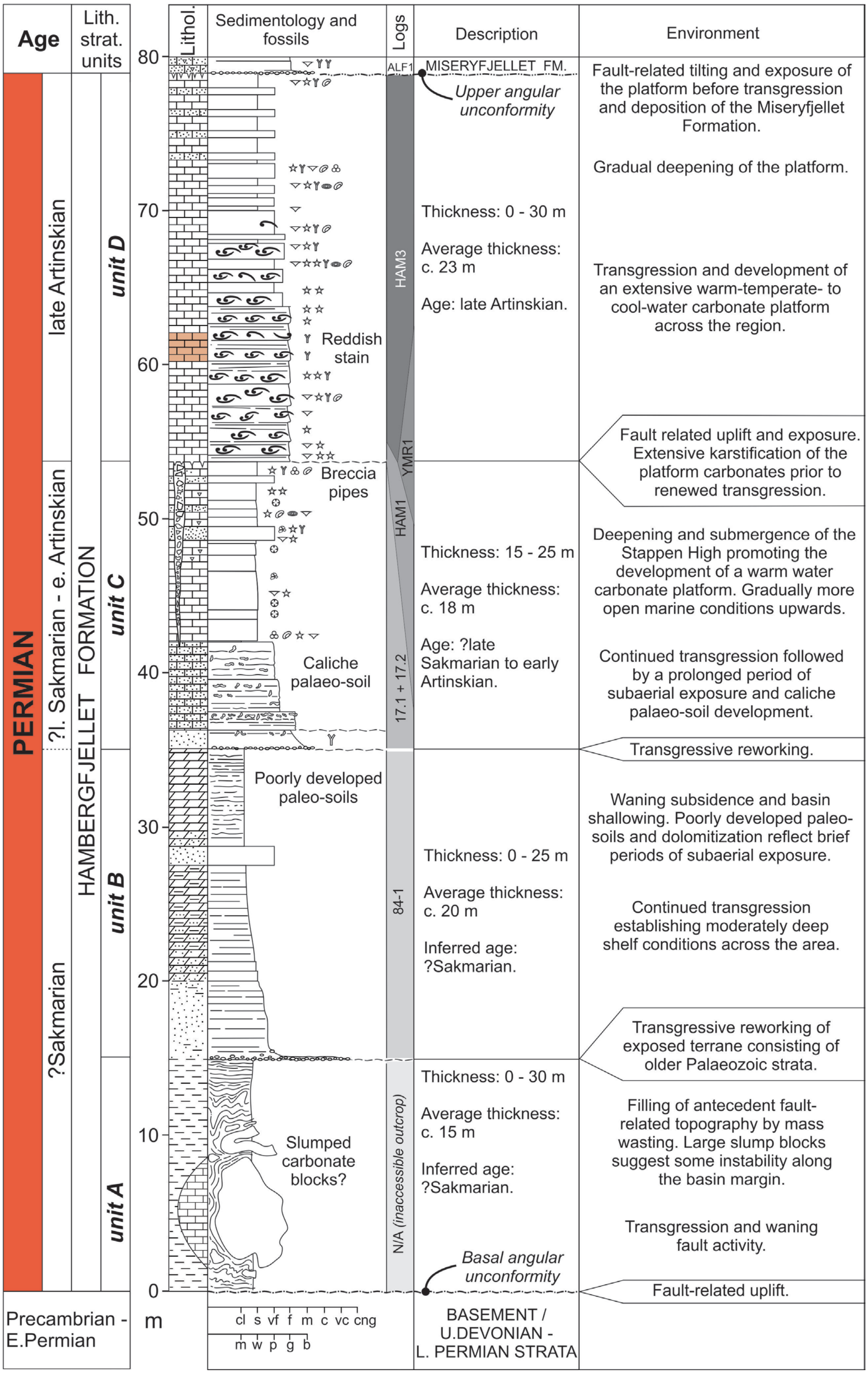

Figure 16. A composite section of the Hambergfjellet Formation based on the field investigations and the microfacies analysis presented in this study. The intervals covered by the logs used to construct the section is indicated. We propose that this section should be referred to as the type section of the unit. See main text for a detailed explanation. Legend is given in Fig. 6.

Alfredfjellet. Unit D has an average thickness of 23 m with a maximum of *c.* 30 m on Fuglefjellet but pinches out rather abruptly west of the Hornvika graben. This gives an accumulative average thickness of *c.* 76 m for our composite section, well within the thickness range presented by previous workers, (*c.* 50 m, Worsley & Edwards, 1976; maximum 50 m, Nakrem et al., 1992; *c.* 60 m, Worsley et al., 2001; up to 70 m, Dallmann et al., 1999; *c.* 100 m, Harland, 1997, see pages 213–214).

The basal boundary of the Hambergfjellet Formation is an angular unconformity which exhibit a highly diachronous and laterally complex nature. This relationship is best viewed at Alfredfjellet where the formation rests unconformably on the steeply dipping strata of the underlying Billefjorden Group. In log 17-1, only unit C is present, here capping the Upper Devonian Røedvika Formation (Figs. 5, 7 & 8A). Laterally, in a northwestward direction, the basal boundary of the formation is defined by the base of unit A, which caps steeply dipping sandstone beds of the lower Carboniferous Nordkapp Formation (Fig. 5B, C). As documented in the 84-1 section at the north-western end of Alfredfjellet, unit B contains a conglomerate at its base and erosively caps a thin sliver of sandstones and carbonate rocks presumably belonging to the Kapp Hanna and the Kapp Dunér formations of the Gipsdalen Group (Simonsen, 1991; Fig. 6).

Unit A of the composite section consists of variously deformed and possibly resedimented carbonate blocks embedded in a dark-coloured mudstone (Figs. 5C & 8C). At Alfredfjellet, neither the 84-1 nor the 17-1 logs document unit A because the unit pinches out to the NW and to the SE. All stratigraphic and sedimentological features are thus based on observations from a distance and tracing on photo mosaics and the digital model (e.g., Figs. 5C & 7A). No age data is available for unit A. However, because it onlaps the lower Permian Kapp Dunér Formation (middle Gzhelian–late Asselian Age; Simonsen, 1991; Dallmann et al., 1999; Worsley et al., 2001), a post ?late Asselian age can be suggested at best.

Unit B is documented by the 84-1 log (Fig. 6). It consists of interbedded siltstone and sandstone beds which gradually fine and transition upwards into alternating dolomitized carbonate mudstone and wackestone beds (Fig. 6). Subordinate sandstone or sandy limestone occur sporadically (Fig. 6). Locally, unit B appears to have a more heterolithic character containing larger amounts of interbedded dark-coloured mudstone, particularly in the central parts of the fault-bounded basins exposed in the coastal cliffs (Figs. 8D & 10). Unit B contains a marked palaeo-soil horizon in its middle part. Because the unit is generally void of any fossils, there are no confirmative age data available. However, a post ?late Asselian to speculative ?Sakmarian age can be suggested based on the age of unit C (see below) and the stratigraphic relationship to unit A (assuming that the proposed post ?late Asselian age is corrects for this unit).

Unit C is documented by the 84-1, 17-1, 17-2, ALF4, HAM1 and YMR1 logs (Fig. 6). It is dominated by thick-bedded mudstone to wackestone and subordinate grainstone beds (Figs. 6, 15 & 16). Sandstone interbeds are abundant in its lower part, particularly at Alfredfjellet where it erosively caps older sandstone-bearing strata (Figs. 5D, 7A & 8A). Faecal pellets, scattered brachiopods, echinoderms, corals, foraminifers, and various bryozoans occur throughout (Fig. 13). Multiple palaeo-soil horizons with well-developed in situ *Microcodium* occur locally, and reworked *Microcodium* aggregates occur sporadically in the upper part of the unit. Corals reported in this part of the formation suggest a late Asselian to Sakmarian age (Fedorowski, 1986), while a preliminary fusulinid study indicates a possible ?late Asselian/?Sakmarian to early Artinskian age (Simonsen, 1991; see also Worsely et al., 2001). In their regional biostratigraphic review of the Permian succession of Svalbard, Nakrem et al. (1992) suggested a ?Sakmarian age for the stratigraphic interval corresponding to our unit C. Based on these considerations, we speculatively suggest a ?late Sakmarian–early Artinskian age for unit C.

Unit D has a sharp, erosive base, and is bounded above by a low-angle angular unconformity demarcated by the basal conglomerates of the Miseryfjellet Formation. Unit D is clearly distinguished from unit C by a sudden increase of sandy, bioclastic brachiopod grainstones, and sandstone-rich bryozoan packstones, as well as moderate silicification, which makes it a cliff-forming unit in the landward-facing outcrops (Figs. 6, 10, 11, 12 & 14). The lower part of unit D has a thick-bedded, massive appearance, with tabular bed geometries (Fig. 14A). The upper part is more thinly bedded with abundant undulating to nodular beds (Fig. 14B). A characteristic red hue is evident in places (Fig. 12C). Conodonts and fusulinids indicate a definite late Artinskian age for unit D (Nakrem, 1991a; Simonsen, 1991; Nakrem et al., 1992).

Discussion

Depositional environments and regional implications

The interrelations of facies in units A, B, and C imply deposition on a shallow, likely warm-water carbonate platform which straddled the Stappen High during the early Permian. The platform developed in a stepwise manner, thus recording the interaction of eustatic sea-level fluctuations and local tectonism before the Stappen High became fully submerged during the ensuing Kungurian transgression. Based on the deformed and chaotic character of unit A, we interpret it to record a period of slumping and mass-transport deposition during or soon after transgression of previously developed fault and/or erosional relief (Fig. 16). Because an outlier of the Kapp Dunér Formation (middle Gzhelian–late Asselian Age) is onlapped by unit A and erosively capped by unit B at Alfredfjellet, the inherited relief must have formed in the earliest Permian, possibly resulting from exposure and deep erosion of the Stappen High during a proposed Sakmarian uplift event (Worsley et al.,2001). The Sakmarian uplift is particularly evident in outcrops on the west coast of Bjørnøya where an erosional unconformity/exposure surface occurs atop the Kapp Dunér Formation (Worsley et al., 2001). We speculate that unit A sits directly on the lateral (southeastward) continuation of this surface on Alfredfjellet. Based on this interpretation, a ?Sakmarian age may thus be suggested for unit A. The localized and patchy distribution of interpreted mass-transport deposits in some of the fault-bounded basins on Fuglefjellet (which we tentatively assign to unit A), may indicate that minor fault movements accompanied the Sakmarian uplift event.

Based on the results from the outcrop investigations and the microfacies analysis, we interpret units B and C to be of a shallow marine origin recording deposition during continued transgression of the area in the ?Sakmarian to ?early Artinskian after the uplift event (Figs. 6, 15 & 16). The inherited erosional relief and the plausible minor fault movements that controlled the development of unit A continued to affect deposition of unit B, although to a much lesser extent. Based on its fine-grained, heterolithic character, unit B may have been deposited under low-energy conditions in slightly deeper waters than unit C (Fig. 16). The thick-bedded, fossiliferous character and constant thickness of unit C, suggests that it represent a laterally extensive, shallow, warm-water carbonate platform deposit. This is also supported by the occurrence of faecal pellets, which are commonly found in subtidal and intertidal environments in warm, shallow marine carbonate-platform settings (Wanless et al. 1981; Flügel, 2004).

Tabulate corals and rugose colonial corals also occur in unit C. In general, Palaeozoic corals are adapted to a soft substrate in warm shelf seas (Scrutton, 1998). As such, we suggest that unit B formed a ?Sakmarian precursor to the warm-water carbonate platform of unit C, which we tentatively assign to the ?Sakmarian to ?early Artinskian. The palaeo-soils documented in both units, and the in situ *Microcodium* horizons occurring in unit C (in the 17-1, HAM1, and YMR1 sections; Fig. 6), indicate recurrent subaerial exposure, foremost governed by local fault movements and variable subsidence rates, and subordinately by glacio-eustatic fluctuations caused by waxing and waning of Gondwana icesheets in the southern hemisphere (e.g., Stemmerik, 2008; Blomeier et al., 2013; Blomeier, 2015).

Collapse breccias are widely known from the Gipsdalen Group carbonate rocks in Spitsbergen, (e.g., Lønøy, 1995; Eliassen & Talbot, 2005), and similar features have been detected in subsurface data from the same stratigraphic interval on the Loppa High (Sayago et al., 2012; Ahlborn et al., 2014). The formation of these breccias has been attributed to dissolution of evaporites during prolonged platform exposure and karstification. In Spitsbergen, such pronounced episodes of exposure occurred in Asselian to Sakmarian times (Eliassen & Talbot, 2005), whereas the Loppa High experienced differential uplift and prolonged exposure from the latest Permian onwards (Stemmerik et al., 1999). Because we find absolutely no evidence of evaporites in the Hambergfjellet Formation and the breccia pipes in unit C are inaccessible, we do not have data that convincingly indicates an origin for these structures, though their proximity to the Alfredfjellet fault may support a structural control. Furthermore, because the breccia pipes in unit C (Fig. 5) co-occur with a karstification surface below the basal boundary of the Miseryfjellet Formation (Fig. 6), it seems natural to link their development to recurrent episodes of fault-controlled tilting and uplift of the Stappen High and prolonged episodes of exposure.

Sporadic and recurrent input of clastic material is recorded in several of the microfacies by the local abundance of quartz grains and the presence of angular lithoclasts. At the macro scale, this is recorded by the occurrence of interbedded sandstones in some places. The clastic input may have resulted from the establishment of transient clastic shoreline systems plastered along exposed terrain, as well as erosion and reworking of older sandstone-bearing strata that were exposed elsewhere on the Stappen High prior to the drowning of the entire region (e.g., Worsley et al., 2001). The abundance of sandstones in the strata sitting above the basal angular unconformity of the formation is thus attributed to transgressive reworking of the underlying sandstone-bearing deposits of the Billefjorden Group.

Deepening of the area continued in the late Artinskian, concurrent with deposition of the bioclastic carbonates of unit D, which, at one point, most likely covered the entire high. Unit D contains fauna elements typical of cool-water carbonate platforms (e.g., brachiopods, echinoderms etc.) and are very similar to the Vøringen Member in Spitsbergen (e.g., Stemmerik, 1997; Uchman et al., 2016). However, the unit also contain fusulinids, which is typical of warm to temperate (i.e., subtropical) water temperatures (e.g., Beauchamp, 1994; Bensing et al., 2008). This indicates mixed warm- and cool-water faunas, which suggests transitional temperatures followed by gradual cooling of the water mass due to increasing water depths, climatic cooling driven by continued northward continental drift, climatic deterioration, or a combination of these factors. Moreover, the fauna elements, which are typical of normal marine and well-oxygenated conditions, and the concomitant lack of features consistent with subaerial exposure within unit D, indicates that the Stappen High was submerged for most of the late Artinskian. This is in line with the transgressive development of the Bjarmeland Group documented elsewhere on the Barents Shelf (e.g., Larssen et al., 2002; Di Lucia et al., 2017; Sayago et al., 2018). The abrupt erosional pinch-out of unit D west of the western boundary fault of the Hornvika graben and the corresponding fault-controlled thickening east of this fault is interesting. It may be a primary depositional feature caused by syn-tectonic deposition resulting in fault-bound bioclastic wedge (as also suggested by Worsley et al., (2001) for the present-day wedge-shaped geometry of the entire formation). A more likely alternative, though, especially given the angular erosional unconformity at the base of the Miseryfjellet Formation in Ymerdalen and the northwestward erosional pinch-out of unit D, is that unit D originally covered a much larger area than its present extent. Tilting and differential subsidence followed by uplift caused erosion of the unit across the footwall block, resulting in the northwestward erosional pinch-out and concomitantly preserving the unit in the eastern and southeastern parts of the present-day mountain massif. A second episode of tilting followed this time towards the SW. Subsequently, the differentially uplifted high was planed off during prolonged exposure, eventually giving rise to the present north- to north-eastward thinning and wedge-shaped geometry of the Hambergfjellet Formation. The breccia pipes observed in unit C developed during this prolonged period of exposure. Collectively, all the above features (i.e., pinch out of unit D, thickness variations, variable dips, breccia pipes etc.) may testify to an early/precursory phase of the late Permian rifting event that occurred west of the Stappen High (Blaich et al., 2017). Finally, after peneplanation, the area was transgressed, and fully marine conditions were yet again re-established across the Stappen High sometime during the middle to late Permian as evidenced by the bryozoan-dominated Miseryfjellet Formation (Worsley et al., 2001; Larssen et al., 2002).

One of the most prominent sedimentological features of unit D is the abundance of brachiopods (Figs. 6, 12, 14 & 16). The brachiopod-dominated beds, mainly consisting of fragmented shells, suggests high energy and frequent reworking of shell banks in an open marine platform setting (e.g., Malkowski & Hoffman, 1979; Ezaki et al., 1994; Blomeier et al., 2013; Uchman et al., 2016). Calmer periods occurred as evidenced by the occurrence of small articulated brachiopods. The deposition of the brachiopod beds may thus have taken place between fair-weather wave base and storm wave base.

Bryozoans are a common constituent of cool-water carbonate platforms and occur abundantly in the Bjarmeland Group on the Barents Shelf and in the Tempelfjorden Group elsewhere, typically forming prominent build-ups (Stemmerik et al., 1999; Stemmerik & Worsley 2000; Worsley et al. 2001; Larssen et al. 2002; Blomeier et al., 2013). The sparse occurrence of bryozoans and the absence of associated build-ups in the Hambergfjellet Formation, as well as the contemporary lack of fusulinids in the Miseryfjellet Formation, is ambiguous. It may point to generally unfavourable conditions for cool-water fauna elements to thrive and dominate, further implying shallow and relatively warm to temperate water conditions across the Stappen High during the Artinskian (e.g., as indicated by the occurrence of fusulinids). In contrast, deeper basins characterized by colder water masses elsewhere on the shelf formed ideal sites for the accumulation of bryozoans. Collectively, this suggests a carbonate platform which developed under the mixed influence of warm to temperate and cold-water masses, presumably controlled by the supra-regional transition from warm to cool water conditions, glacio-eustatic sea-level fluctuations, and superimposed, local physiographic factors including tectonism.

Notes on the stratigraphic development and correlations to Spitsbergen

Correlation of the Hambergfjellet Formation to time-equivalent strata on Spitsbergen has been discussed on several occasions (e.g., Nakrem, 1991b; Nakrem et al., 1992; Worsley et al., 2001; Larssen et al., 2002; Samuelsberg et al., 2003; Stemmerik and Worsley, 2005; Sorento et al., 2020). However, the uncertain and variable age assignments proposed for the Hambergfjellet Formation have hampered detailed correlations. Gobbett (1963) investigated brachiopods in the downfaulted block in Ymerdalen and suggested a Sakmarian age for the formation, whereas Fedorowski (1986) suggested an Asselian to Sakmarian age based on the rugose coral assemblage. From the study of conodonts from a section at the eastern slopes of Hambergfjellet (corresponding to the combined HAM1 and HAM3 sections of this study; Figs. 6 & 11C, D), Nakrem (1991a) assigned a late Artinskian age for the upper part of the formation (our unit D), and a speculative ?Sakmarian age for the underlying part (our unit C). He also noted great similarities between “the upper part” of the Hambergfjellet Formation (our unit D) and the upper Artinskian Vøringen Member at the base of the Tempelfjorden Group in Spitsbergen.

Based on various fossil faunas, including conodonts and fusulinids, the Hambergfjellet Formation was eventually assigned a Sakmarian to late Artinskian age by Nakrem et al. (1992), implying correlation to the upper part of the Gipshuken Formation (Sakmarian–Artinskian; Gipsdalen Group) and the Vøringen Member (late Artinskian) in Spitsbergen.

In Spitsbergen, the upper part of the Gipshuken Formation contains bioclastic carbonate rocks with a faunal assemblage consistent with a mixed open marine and peritidal platform to supratidal sabkha environment (e.g., Blomeier et al., 2011; Sorento et al., 2020). These locally bioclastic-rich carbonate rocks rest erosively on top of a thick succession of dolostones and evaporites constituting the lower Gipshuken Formation (e.g., Hüneke et al., 2001; Blomeier et al., 2011; Sorento et al., 2020). Several studies have reported an abrupt regional facies change from warm-water carbonates in the upper Gipshuken Formation to cool-water carbonates in the Vøringen Member of the Kapp Starostin Formation (e.g., Hüneke et al., 2001; Blomeier et al., 2011, 2013; Uchman et al., 2016). We tentatively suggest that our units A to C correlate to the upper parts of the Gipshuken Formation, possibly representing a condensed and lateral-distal facies equivalent of the Skansdalen and Templet members.

The Vøringen Member, which is a brachiopod-dominated bioclastic limestone unit on Spitsbergen, accumulated during a regional transgression of the shallow and periodically exposed warm-water carbonate platform of the Gipsdalen Group during the late Artinskian (e.g., Blomeier et al., 2011; Uchman et al., 2016; Sorento et al., 2020). In their facies model of the unit, Blomeier et al. (2011) suggested that warm-water conditions prevailed in the inner platforms during the late Sakmarian to early Artinskian, whereas cool-water fauna elements devoid of fusulinids were introduced by gradual deepening during the late Artinskian transgression as colder water masses protruded the shallow platform. We envisage a similar development on the Stappen High during the late Artinskian. Thus, because of the great facies similarities and corresponding age assignments (based on conodonts, Nakrem, 1991a; Nakrem et al., 1992), we suggest that the Vøringen Member and our unit D are in fact correlative and laterally equivalent units. However, the lack of fusulinids in the Vøringen Member indicates somewhat cooler conditions further north on the platform, either being a result of Spitsbergen's location some few hundred kilometres north of Bjørnøya (i.e., a natural northerly cooling), or local physiographical conditions.

Possible offshore correlations and tectonostratigraphic implications

Offshore, the Bjarmeland Group is significantly thicker than on Bjørnøya (>400 m vs. <100 m), and includes various build-ups dominated by heterozoan biota such as bryozoans and *Tubiphytes*, as well as inter-reef carbonate mudstones (Larssen et al., 2002; Colpaert et al., 2007; Di Lucia et al., 2017). Such build-ups, which form in relative deep waters and in areas of high subsidence rates (e.g., near major fault zones), have not been observed in the Hambergfjellet Formation, presumably testifying to the overall shallower and warmer water conditions that prevailed across the Stappen High in comparison to the deep basins.

The lower to middle parts of the Bjarmeland Group, assigned to the Ulv Formation (middle Sakmarian–Artinskian), is 60–210 m thick, and consists of dark, fine-grained limestones, silty limestones, and shales deposited in relatively deep shelf environments (Larssen et al., 2002). This unit may be a lateral distal correlative of the upper part of the Gipshuken Formation on Spitsbergen (Larssen et al., 2002). Based on age and facies similarities, we speculate that our units A to C may be the nearshore equivalent to the Ulv Formation. However, features consistent with subaerial exposure, as documented in units B and C, have not been reported in the Ulv Formation.

In the offshore basins, the upper part of the Bjarmeland Group is assigned to the Isbjørn Formation (middle Sakmarian–late Artinskian) and have tentatively been correlated to the Vøringen Member on Spitsbergen. The Isbjørn Formation is 10–90 m thick and consists of bioclastic carbonate rocks dominated by bryozoans and crinoids, which record deposition in moderately deep, inner shelf settings (Di Lucia et al., 2017). The unit is widespread and records deposition during the regional transgression in the late Artinskian. Dark-coloured, silty wackestones, which resemble those of the Ulv Formation, locally interfinger with the bioclastics and record deposition in deeper waters. In terms of the assigned age and partly the reported facies, we suggest that our unit D is a condensed equivalent of the Isbjørn Formation, and thus correspond to the Vøringen Member on Spitsbergen. An alternative interpretation is that all our four units correspond to the Isbjørn Formation, recording internal heterogeneities. Whereas the dominance of bryozoans in the Isbjørn Formation is attributed to deep water on the shelf, the dominance of brachiopods over bryozoans, as well as the sporadic occurrence of fusulinids in unit D indicate deposition at warmer and shallower water depths under higher energetic conditions across the Stappen High. The regional transgression which eventually drowned the Stappen High during the late Artinskian, appears to be the main cause of the change to a cool-water biota in the study area. The closure of the Uralian seaway during the early–late Permian may also have influenced this development, eventually inhibiting warm water fauna from the Palaeotethys to enter the Boreal region (Worsley, 2008). The dominance of bryozoans and other cool-water biota in the Miseryfjellet Formation indicates continued deepening and submergence of the Stappen High in the late Permian. Given that similar facies changes are reported from the upper Palaeozoic successions in the Canadian Arctic (Beauchamp & Henderson, 1994; Reid et al. 2007) and in NE Greenland (Stemmerik, 1997), it appears that glacio-eustacy, northward continental drift, and climatic deterioration, as well as local tectonics, all influenced the evolution this circum-Arctic, epicontinental, warm-temperate- to cool-water carbonate platform.

A similar stratigraphic development to that recorded on Bjørnøya, with strata onlapping and thinning across structural highs, is noted for the Bjarmeland Group in the offshore basins (e.g., Larssen et al., 2002). The basal unconformity of the Bjarmeland Group is highly diachronous, being oldest in the deeper basins and youngest on the platforms, thus resembling the documented composite nature of the basal angular unconformity of the Hambergfjellet Formation. The presence of faults and prominent fault-bounded basins in the southernmost part of Bjørnøya is intriguing (Fig. 17). Most of the faults in the underlying basement do not affect the Hambergfjellet Formation (e.g., the Skrøslingen fault, Figs. 9 & 10), and presumably record Carboniferous faulting (e.g., Worsley et al., 2001). Only some few faults seem to solely affect the Hambergfjellet Formation (Figs. 9 & 10). The Alfredfjellet fault is by far the best example and cuts units A to C before it terminates against the basal surface of the Miseryfjellet Formation (Figs. 5 & 17). This presumably indicates ?Sakmarian to ?early Artinskian minor fault activity which predates the well-known late Permian faulting event along the western Barents Shelf margin (e.g., Faleide et al., 1984; Blaich et al., 2017; Fig. 2). In addition, small faults which only affect unit D indicate some very minor (extensional) tectonic activity during the late Artinskian. Several other faults offset both the Hambergfjellet and Miseryfjellet formations, presumably recording Mesozoic faulting and/or reactivation of Palaeozoic lineaments (Fig. 17). Episodes of rifting west of the Stappen High is known from the Early Triassic, Late Jurassic and Early Cretaceous (Blaich et al., 2017).

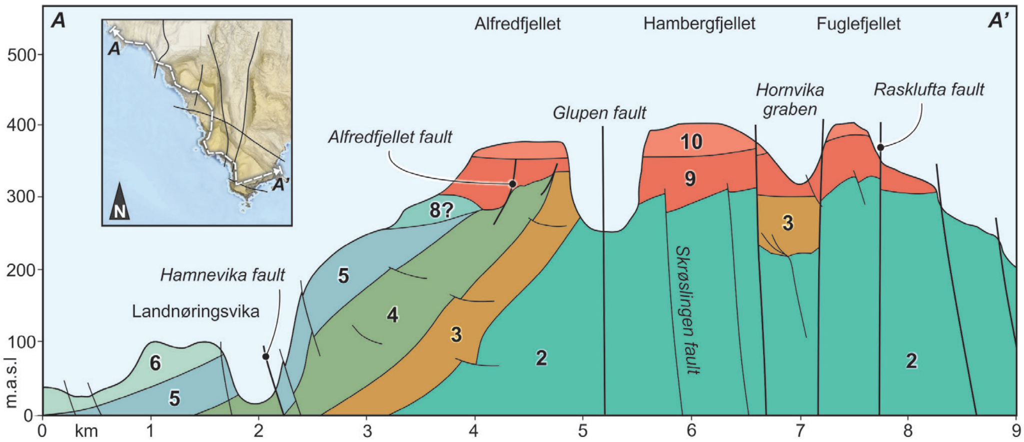

Figure 17. Conceptual cross-section summarizing the tectono-stratigraphic setting of southern Bjørnøya. Faulting was generally not pronounced during deposition of the Hambergfjellet Formation (the unit marked with number 9). However, the Alfredfjellet fault appears to offset the Hambergfjellet Formation and extend down into the underlying strata. It does not affect the overlying middle Permian Miseryfjellet Formation (unit 10). In combination with the occurrence of minor syn-sedimentary faults in unit D of the Hambergfjellet Formation, this indicates tectonic activity prior to the late Permian rifting event west of the Stappen High. The boundary faults of the Hornvika graben and the Rasklufta fault (including all their smaller conjugate faults) offset both the Hambergfjellet and the Miseryfjellet formations and extend into the underlying basement. These faults are attributed to Mesozoic structuring events. Other faults, such as the Skrøslingen fault, do not appear to influence the Hambergfjellet Formation. The thickening of the formation near these faults rather seems to be a result of infilling and healing of antecedent topography possibly formed during Sakmarian uplift and erosion and minor fault activity. Colour legend is provided in Fig. 1.

Conclusions

This study presents a detailed stratigraphic analysis of the lower Permian Hambergfjellet Formation (?Sakmarian to late Artinskian Age) on Bjørnøya – the only exposed part of the Bjarmeland Group carbonate platform strata. We present a composite type section for the Hambergfjellet Formation and recognize four internal units (units A to D), which collectively record a complex stratigraphic development influenced by early Permian tectonism and relative sea-level fluctuations, as well as antecedent topography created during earlier structuring events.

• Units A and B (post ?late Asselian to ?Sakmarian Age) are restricted to a series of fault-bounded basins in the very south of the island where they onlap and partly thin across rotated basement fault blocks, and apparently fill in antecedent topography possibly created during Sakmarian uplift and erosion of the Stappen High. The facies characteristics of units A and B are generally consistent with shallow marine deposition during the ensuing transgression, whereas distorted and chaotically bedded strata in unit A indicate that slumping was important an process during the initial phase of infilling.

• Unit C (?Sakmarian–?early Artinskian Age) is a thick-bedded, sheet-like, micrite-rich limestone unit which has a constant thickness across the entire outcrop belt. It contains abundant faecal pellets and fauna elements such as foraminifera, corals, subordinate ostracods, and bryozoans, generally indicative of deposition on a shallow, warm-water carbonate platform. Horizons of *Microcodium* and poorly developed palaeo-soils indicate periodic subaerial exposure. The local abundance of sandstones in the lower part indicates transgressive reworking of underlying sandstone-bearing strata of the Billefjorden Group, whereas the gradual loss of sandstones upwards is attributable to an overall transgressive development for unit C.

• Unit D (late Artinskian Age) consists of brachiopod-dominated, fusulinid-bearing bioclastics deposited on a shallow, fully marine, warm-temperate- to cool-water carbonate platform. The development of this platform appears to coincide with a supra-regional, circum-Arctic transgression in the late Artinskian. As such, we consider unit D and the Vøringen Member at the base of the Tempelfjorden Group on Spitsbergen to be correlative and laterally equivalent units. Build-ups of bryozoans and Tubiphytes such as those reported in the Bjarmeland Group offshore, are not documented in the Hambergfjellet Formation, reflecting shallower waters across the Stappen High than in the nearby offshore basins throughout the Artinskian.

• The Stappen High must have been influenced by several episodes of differential uplift and minor fault movements during the late Artinskian, which concomitantly caused exposure and karstification of the carbonate platform prior to peneplanation and deposition of the Miseryfjellet Formation (Kungurian–Wordian Age). This is evident by internal dip-variations and an abrupt pinch-out of unit D to the west/northwest, the north- to northeastward wedging of the entire Hambergfjellet Formation, the laterally extensive karstification surface in the top of the formation, and breccia pipes in unit C. In addition, the presence of angular and highly diachronous unconformities at the base and top of the Hambergfjellet Formation, a series of small grabens, and at least one normal fault with inferred drag-folds which involve parts of the Hambergfjellet Formation, indicate local tectonism pre-dating the well-known late Permian extensional event along the western Barents Shelf margin.

Acknowledgements. We are grateful for financial support from the Norwegian Petroleum Directorate and Lundin Norway AS. We also extend our deepest gratitude to the crew members and captains of both Stålbas *and* Youexplore*, this project would not have been possible to accomplish without their professional and safe operations. Fredrik Wesenlund is kindly thanked for valuable field assistance in 2017. Valuable photos have kindly been provided by Lars Johan Ersland (picture in Fig. 9C) and Vetle Nilsen Malmberg (pictures in Figs. 5A, 9A, 10A & 10D). SAG received funding from the Suprabasin project which is funded by the Research Council of Norway (grant number 295208). We deeply appreciate constructive and clarifying referee comments from Hans Arne Nakrem and Lars Stemmerik.*

References

Adams, A. & Mackenzie, W. 1998: *A Colour Atlas of Carbonate Sediments and Rocks Under the Microscope.* Manson Publishing, London, 180 pp. https://doi.org/10.1201/9781840765403

Ahlborn, M. & Stemmerik, L. 2015: Depositional evolution of the Upper Carboniferous – Lower Permian Wordiekammen carbonate platform, Nordfjorden High, central Spitsbergen, Arctic Norway. *Norwegian Journal of Geology 95*, 91–126. https://doi.org/10.17850/njg95-1-03

Ahlborn, M., Stemmerik, L. & Kalstø, T.K. 2014: 3D seismic analysis of karstified interbedded carbonates and evaporites, Lower Permian Gipsdalen Group, Loppa High, southwestern Barents Sea. *Marine and Petroleum Geology 56*, 16–33. https://doi.org/10.1016/j.marpetgeo.2014.02.015

Andersson, J.G. 1899: Über die Stratigraphie und Tektonik den Bären Insel. *Bulletin of the Geological Institution of the University of Upsala 4*, 243–280.

Bathurst, R.G. 1971: *Carbonate sediments and their diagenesis*. Elsevier publishing company, Ams terdam, 620 pp.

Beauchamp, D. 1994: Permian climatic cooling in the Canadian Arctic. *In* Klein, G.O. (Ed.) Pangea: *Paleoclimate, Tectonics, and Sedimentation During Accretion, Zenith, and Breakup of a Supercontinent*. Geological Society of America Special Papers 288, pp. 229–245. https://doi.org/10.1130/SPE288-p229

Beauchamp, B. & Henderson, C.M. 1994: The Lower Permian Raanes, Great Bear Cape and Trappers Cove formations, Sverdrup Basin, Canadian Arctic: stratigraphy and conodont zonation. *Bulletin of Canadian Petroleum Geology 42,* 562–597.

Beauchamp, B. & Desrochers, A. 1997: *Permian warm- to very cold-water carbonates and cherts in northwest Pangea. In* James, N.P. & Clarke, J.A.D. (eds.): *Cool-water Carbonates.* Society for Sedimentary Geology Special Publication 56, Tulsa, Oklahoma, USA, pp. 327–347. https://doi.org/10.2110/pec.97.56.0327

Bensing, J.P., James, N.P. & Beauchamp, B. 2008: Carbonate deposition during a time of mid-latitude ocean cooling: Early Permian subtropical sedimentation in the Sverdrup Basin, Arctic Canada. *Journal of Sedimentary Research 78*, 2–15. https://doi.org/10.2110/jsr.2008.004

Blaich, O.A., Tsikalas, F. & Faleide, J.I. 2017: New insights into the tectono-stratigraphic evolution of the southern Stappen High and its transition to Bjørnøya Basin, SW Barents Sea. *Marine and Petroleum Geology 85*, 89–105. https://doi.org/10.1016/j.marpetgeo.2017.04.015

Blomeier, D., Dustira, A., Forke, H. & Scheibner, C. 2011: Environmental change in the Early Permian of NE Svalbard: from a warm-water carbonate platform Gipshuken Formation to a temperate, mixed siliciclastic-carbonate ramp Kapp Starostin Formation. *Facies 57*, 493–523. https://doi.org/10.1007/s10347-010-0243-z

Blomeier, D., Dustira, A.M., Forke, H. & Scheibner, C. 2013: Facies analysis and depositional environments of a storm-dominated, temperate to cold, mixed siliceous-carbonate ramp: the Permian Kapp Starostin Formation in NE Svalbard. *Norwegian Journal of Geology 93*, 75–93.

Blomeier, D. 2015: Chapter 6: Historical geology - Permian. *In* Dallmann, W. (Ed.) *Geoscience Atlas of Svalbard*. Norsk Polarinstitutt Rapportserie 148, pp. 110–113.

Buckley, S.J., Ringdal, K., Naumann, N., Dolva, B., Kurz, T.H., Howell, J.A. & Dewez, T.J.B. 2019: LIME: Software for 3-D visualization, interpretation, and communication of virtual geoscience models. *Geosphere 15*, 222–235. https://doi.org/10.1130/GES02002.1

Bugge, T., Mangerud, G., Elvebakk, G., Mørk, A., Nilsson, I., Fanavoll, S. & Vigran, J.O. 1995: The upper Paleozoic succession on the Finnmark Platform, Barents Sea. *Norwegian Journal of Geology 75,* 3–30.

Colpaert, A., Pickard, N., Mienert, J., Henriksen, L. B., Rafaelsen, B. & Andreassen, K. 2007: 3D seismic analysis of an Upper Paleozoic carbonate succession of the Eastern Finnmark Platform area, Norwegian Barents Sea. *Sedimentary Geology 197*, 79–98. https://doi.org/10.1016/j.sedgeo.2006.09.001

Cutbill, J. & Challinor, A. 1965: Revision of the stratigraphical scheme for the Carboniferous and Permian rocks of Spitsbergen and Bjørnøya. *Geological Magazine 1025*, 418–439. https://doi.org/10.1017/S0016756800053693

Dallmann, W.K. & Krasil'ščikov, A.A. 1996: Geological map of Svalbard, sheet D20G Bjørnøya, scale 1:50 000. *Norsk Polarinstitutt.*

Dallmann, W.K., Gjelberg, J.G., Harland, W.B., Johannessen, E.P., Keilen, H.B., Lønøy, A., Nilsson, I. & Worsley, D. 1999: Upper Palaeozoic lithostratigraphy. *In* Dallmann, W.K. (ed.): *Lithostratigraphic lexicon of Svalbard*. Norsk Polarinstitutt, Tromsø, pp. 25–126.

Di Lucia, M., Sayago, J., Frijia, G., Cotti, A., Sitta, A. & Mutti, M. 2017: Facies and Seismic analysis of the Late Carboniferous–Early Permian Finnmark carbonate platform (southern Norwegian Barents Sea): An assessment of the carbonate factories and depositional geometries. *Marine and Petroleum Geology 79,* 372–393. https://doi.org/10.1016/j.marpetgeo.2016.10.029

Dunham, R.J. 1962: Classification of carbonate rocks according to depositional texture. *In* Ham, W.E. (ed.): *Classification of carbonate rocks*. American Association of Petroleum Geologists Memoir 1, pp. 108–171. https://doi.org/10.1306/M1357

Eliassen, A. & Talbot, M.R. 2005: Solution-collapse breccias of the Minkinfjellet and Wordiekammen Formations, central Spitsbergen, Svalbard: a large gypsum palaeokarst system. *Sedimentology 52,* 775–794. https://doi.org/10.1111/j.1365-3091.2005.00731.x

Ezaki, Y., Kawamura, T. & Nakamura, K. 1994: Kapp Starostin Formation in Spitsbergen: A sedimentary and faunal record of Late Permian palaeoenvironments in an Arctic region. *Canadien Society of Petroleum Geologists Memoir 17,* 647–655.

Faleide, J.I., Gudlaugsson, S.T. & Jacquart, G. 1984: Evolution of the western Barents Sea. *Marine and Petroleum Geology 1*, 123–150. https://doi.org/10.1016/0264-8172(84)90082-5

Fedorowski, J. 1986: The rugose coral faunas of the Carboniferous/Permian boundary interval. *Acta Palaeontologica Polonica 31,* 253–275.

Flügel, E. 2004. *Microfacies of carbonate rocks*. Springer-Verlag, Berlin Heidelberg, 976 pp. https://doi.org/10.1007/978-3-662-08726-8

Gobbett, D.J. 1963: Carboniferous and Permian brachiopods of Svalbard. *Norsk Polarinstitutt Skrifter 127*, 201 pp.

Gudlaugsson, S.T., Faleide, J.I., Johansen, S.E. & Breivik, A.J. 1998. Late Palaeozoic structural development of the South-western Barents Sea. *Marine and Petroleum Geology 15,* 73–102. https://doi.org/10.1016/S0264-8172(97)00048-2

Hanken, N.-M. 1981: *Identifikasjon av fossilfragmenter i tynnslip.* The University of Tromsø, Tromsø, course notes, 97 pp.

Hanken, N.-M., Bjørlykke, K. & Nielsen, J. 2010: Carbonate Sediments. *In* Bjørlykke, K. (ed.): *Petroleum Geoscience: From Sedimentary Environments to Rock Physics.* Springer-Verlag Berlin Heidelberg, pp. 141–200. https://doi.org/10.1007/978-3-642-02332-3_5

Harland, W.B. 1997: The geology of Svalbard. *Geological Society, London, Memoirs 17*, 521 pp. https://doi.org/10.1144/GSL.MEM.1997.017.01.01

Henriksen, E., Ryseth, A.E., Larssen, G.B., Heide, T., Rønning K., Sollid, K. & Stoupakova, A.V. 2011: Tectonostratigraphy of the greater Barents Sea: Implications for petroleum systems. *In* Spencer, A.M., Embry, A.F., Gautier, D.L., Stoupakova, A.V. & Sørensen, K. (eds.): *Arctic Petroleum Geology*. Geological Society of London Memoirs 35, pp. 163–195. https://doi.org/10.1144/M35.10

Holtedahl, O. 1920: On the Palaeozoic Series of Bear Island, especially on the Hecla Hoek system. *Norwegian Journal of Geology 5*, 121–148.

Horn, G. & Orvin, A.K. 1928: Geology of Bear Island: with special reference to the coal deposits, and with an account of the history of the island. *Skrifter om Svalbard og Ishavet 15,* 152 pp.

Hüneke, H., Joachimski, M., Buggisch, W. & Lützner, H. 2001: Marine Carbonate Facies in Response to Climate and Nutrient Level: The Upper Carboniferous and Permian of Central Spitsbergen (Svalbard). *Facies 45*, 93–136. https://doi.org/10.1007/BF02668107

Kabanov, P., Anadón, P. & Krumbein, W.E. 2008: Microcodium: an extensive review and a proposed non-rhizogenic biologically induced origin for its formation. *Sedimentary Geology 205*, 79–99. https://doi.org/10.1016/j.sedgeo.2008.02.003

Larssen, G., Elvebakk, G., Henriksen, L.B., Kristensen, S., Nilsson, I., Samuelsberg, T., Svånå, T., Stemmerik, L. & Worsley, D. 2002: Upper Palaeozoic lithostratigraphy of the Southern Norwegian Barents Sea. *Norwegian Petroleum Directorate Bulletin 9*, 1–76.

Lønøy, A. 1995: A Mid-Carboniferous, carbonate-dominated platform, Central Spitsbergen. Norwegian Journal of Geology 75, 48–63.

Malkowski, K., & Hoffman, A. 1979: Semi-quantitative facies model for the Kapp Starostin Formation (Permian), Spitsbergen. *Acta Palaeontologica Polonica 24*, 217–230.

Nakrem, H.A. 1991a: Conodonts from the Permian succession of Bjørnøya, Svalbard. *Norwegian Journal of Geology 71*, 235–248.

Nakrem, H.A., 1991b: Distribution of bryozoans in the Permian succession of Svalbard (preliminary data). *In* Bigey, F.P. & d'Hondt, J.L. (eds.): *Bryozoa Living and Fossils.* Bulletin de la Socièté des Sciences Naturelles del'Ouest de la France, Mèmoire HS 1, pp. 291–298.

Nakrem, H.A. 1994: Middle Carboniferous-Lower Permian bryozoans from Spitsbergen. *Acta Palaeontologica Polonica 39,* 45–116

Nakrem, H.A., Nilsson, I. & Mangerud, G. 1992: Permian Biostratigraphy of Svalbard (Arctic Norway) - A review. *International Geological Reviews 34*, 933–959. https://doi.org/10.1080/00206819209465645

Reid, C.M., James, N.P., Beauchamp, B. & Kyser, T.K. 2007: Faunal turnover and changing oceanography: Late palaeozoic warm-to-cool water carbonates, Sverdrup Basin, Canadian Arctic Archipelago. *Palaeogeography, Palaeoclimatology, Palaeoecology 249*, 128–159. https://doi.org/10.1016/j.palaeo.2007.01.007

Ritter, U., Duddy, I., Mørk, A., Johansen, H. & Dalland, A. 1996: Temperature and uplift history of Bjørnøya (Bear Island), Barents Sea. *Petroleum Geoscience 2,* 133–144. https://doi.org/10.1144/petgeo.2.2.133

Samuelsberg, T.J., Elvebakk, G. & Stemmerik, L. 2003: Late Palaeozoic evolution of the Finnmark Platform, southern Norwegian Barents Sea. *Norwegian Journal of Geology 83*, 351–362.

Sayago, J., Di Lucia, M., Mutti, M., Cotti, A., Sitta, A., Broberg, K., Przybylo, A., Buonaguro, R. & Zimina, O. 2012: Characterization of a deeply buried paleokarst terrain in the Loppa High using core data and multiattribute seismic facies classification. *The American Association of Petroleum Geologists Bulletin 96*, 1843–1866. https://doi.org/10.1306/02271211137

Sayago, J., Di Lucia, M., Mutti, M., Sitta, A., Cotti, A. & Frija, G. 2018: Late Paleozoic seismic sequence stratigraphy and paleogeography of the paleo-Loppa High in the Norwegian Barents Sea. *Marine and Petroleum Geology 97*, 192–208. https://doi.org/10.1016/j.marpetgeo.2018.05.038

Scholle, P.A. 1998: *A color illustrated guide to carbonate rock constituents' textures cements and porosities.* The American Association of Petroleum Geologists Memoir 27, Tulsa, Oklahoma. 241 pp.

Scrutton, C.T. 1998: The Palaeozoic corals, II: structure, variation and palaeoecology. *Proceedings of the Yorkshire Geological Society 52*, 1–57. https://doi.org/10.1144/pygs.52.1.1

Simonsen, B.T. 1991: A biostratigraphic analysis of Upper Palaeozoic fusulinids on Bjørnøya, Svalbard (title translated from Norwegian). Unpublished thesis.

Smelror, M., Petrov, O.V., Larssen, G.B. & Werner, S. 2009: Geological history of the Barents Sea. Geological Survey of Norway, Trondheim, Norway, 138 pp.

Sorento, T., Olaussen, S. & Stemmerik, L. 2020: Controls on deposition of shallow marine carbonates and evaporates–Lower Permian Gipshuken Formation, Central Spitsbergen, Arctic Norway. *Sedimentology 67*, 207–238. https://doi.org/10.1111/sed.12640

Steel, R.J. & Worsley, D. 1984: Svalbard's post-Caledonian strata – an atlas of sedimentational patterns and palaeogeographical evolution. *In* Spencer, A.M., Holter, E., Johnsen, S.O., Mørk, A., Nysæther, E., Songstad, P. & Spinnangr, Å. (eds.): *Petroleum Geology of the North European Margin*. Norwegian Petroleum Society, Graham and Trotman, London, pp. 109–135. https://doi.org/10.1007/978-94-009-5626-1_9

Stemmerik, L. 1997: Permian (Artinskian-Kazanian) cool-water carbonates in North Greenland, Svalbard, and the western Barents Sea. *In* James, N.P., Clarke, J.A.D. (eds.): Cool-water Carbonates. Society of Economic Paleontologists and Mineralogists Special Publication 56, pp. 349–364. https://doi.org/10.2110/pec.97.56.0349

Stemmerik, L. 2008: Influence of late Paleozoic Gondwana glaciations on the depositional evolution of the northern Pangean shelf, North Greenland, Svalbard, and the Barents Sea. *In* Fielding, C.R., Frank, T.D. & Isbell, J.L. (eds.) *Resolving the late Paleozoic ice age in time and space.* Geological Society of America Special Paper 441, pp. 205–217. https://doi.org/10.1130/2008.2441(14)

Stemmerik, L. & Worsley, D. 2000: Upper Carboniferous cyclic shelf deposits, Kapp Kåre Formation, Bjørnøya, Svalbard: response to high frequency, high amplitude sea level fluctuations and local tectonism. *Polar Research 19,* 227–249. https://doi.org/10.3402/polar.v19i2.6548

Stemmerik, L. & Worsley, D. 2005: 30 years on – Arctic Upper Palaeozoic stratigraphy, depositional evolution, and hydrocarbon prospectivity. *Norwegian Journal of Geology 85*, 151–168.

Stemmerik, L., Elvebakk, G. & Worsley, D. 1999: Upper Paleozoic carbonate reservoirs on the Norwegian Arctic Shelf: Delineation of reservoir models with application to the Loppa High. *Petroleum Geoscience 5,* 173–187. https://doi.org/10.1144/petgeo.5.2.173

Uchman, A., Hanken, N.M., Nielsen, J. K., Grundvåg, S-A. & Piasecki, S. 2016: Depositional environment, ichnological features and oxygenation of Permian to earliest Triassic marine sediments in central Spitsbergen, Svalbard. *Polar Research 35.* https://doi.org/10.3402/polar.v35.24782

Walderhaug, O. 1994: Temperatures of quartz cementation in Jurassic sandstones from the Norwegian continental shelf – Evidence from fluid inclusions. *Journal of Sedimentary Research 64*, 311–323. https://doi.org/10.1306/D4267D89-2B26-11D7-8648000102C1865D

Wanless, H.R., Burton, E.A. & Dravis, J. 1981: Hydrodynamics of carbonate fecal pellets. *Journal of Sedimentary Research 51*, 27–36. https://doi.org/10.1306/212F7BFD-2B24-11D7-8648000102C1865D

Worsley, D. 2008: The post-Caledonian development of Svalbard and the western Barents Sea. *Polar Research 27*, 298–317. https://doi.org/10.1111/j.1751-8369.2008.00085.x

Worsley, D., Agdestein, T., Gjelberg, J.G., Kirkemo, K., Mørk, A., Nilsson, I., Olaussen, S., Steel, R.J. & Stemmerik, L. 2001: The geological evolution of Bjørnøya, Arctic Norway: implications for the Barents Shelf. *Norwegian Journal of Geology 81,* 195–234.

Worsley, D. & Edwards, M. 1976: The Upper Palaeozoic succession of Bjørnøya. *Norsk Polarinstitutt Årbok 1974*, 17–34.